Reliability analysis of randomly excited FE modelled structures with interval mass and stiffness via sensitivity analysis

# Reliability Analysis of Randomly Excited FE Modelled Structures with Interval Mass and Stiffness via Sensitivity Analysis

**Alba Sofi[1,*], Filippo Giunta[2], Giuseppe Muscolino[3]**

[1]Department of Architecture and Territory (dArTe), University "Mediterranea" of Reggio Calabria, Inter-University Centre of Theoretical and Experimental Dynamics
Via dell'Università 25, 89124 Reggio Calabria, Italy
e-mail: alba.sofi@unirc.it

[2]Department of Engineering Structures, Section of Mechanics and Physics of Structures (MPS), Faculty of Civil Engineering and Geosciences, Delft University of Technology
Stevinweg 1, 2628 Delft, Netherlands
e-mail: f.giunta@tudelft.nl

[3]Department of Engineering, University of Messina, Inter-University Centre of Theoretical and Experimental Dynamics
Villaggio S. Agata, 98166 Messina, Italy
e-mail: gmuscolino@unime.it

## Abstract

The present study focuses on reliability analysis of linear discretized structures with uncertain mass and stiffness parameters subjected to stationary Gaussian multi-correlated random excitation. Under the assumption that available information on the uncertain parameters is poor or incomplete, the interval model of uncertainty is adopted. The reliability function for the *extreme value* stress process is evaluated in the framework of the *first-passage* theory. Such a function turns out to have an interval nature due to the uncertainty affecting structural parameters. The aim of the analysis is the evaluation of the bounds of the *interval reliability function* which provide a range of structural performance useful for design purposes. To limit detrimental overestimation caused by the *dependency phenomenon*, a sensitivity-based procedure is applied. The main advantage of this approach is the capability of providing appropriate combinations of the endpoints of the uncertain parameters which yield accurate estimates of the bounds of the *interval reliability function* for the *extreme value* stress process as long as monotonic problems are dealt with. Two case studies are analyzed to demonstrate the accuracy and efficiency of the presented method.

**Keywords:** Random excitation; Uncertain parameters; Interval reliability function; Interval analysis; Sensitivity analysis.

*Corresponding author

## 1. INTRODUCTION

The actual values of parameters involved in any engineering design are affected by several sources of uncertainties ensuing from manufacturing inaccuracies, model or measurement errors etc. (see e.g., [1]-[3]). Such uncertainties have been traditionally incorporated into structural reliability analysis using well-established probabilistic approaches. Failure probabilities are highly sensitive to the assumed probabilistic distribution of input parameters, especially in the tails [4],[5]. This entails that the outcomes of the classical probabilistic reliability analysis may be considered accurate as long as sufficient information is available to define the probability density function of the uncertain parameters. If only vague, incomplete or fragmentary data are available, the use of non-probabilistic approaches (see e.g., [6],[7]) is deemed more appropriate to retrieve reliable predictions of the safety level. This issue has been first addressed by Ben-Haim [4] who introduced a non-probabilistic concept of reliability in the context of the convex model of uncertainty. The underlying idea was to define a range of structural performance rather than deriving a single value of the failure probability.

The awareness of possible limitations of traditional probabilistic methods [8] has motivated the use of non-probabilistic uncertainty descriptions, such as the interval model [9],[10], convex models [11] or fuzzy-sets [12], in conjunction with classical methods for structural reliability analysis (see e.g.,[13]-[27]) and reliability-based optimization (see e.g.[28],[29]). Over the last decade, several studies have also been devoted to structural safety assessment in the presence of hybrid uncertainties, i.e. aleatory and epistemic (see e.g., [30]-[35]).

Besides the unavoidable uncertainty of design parameters, another key factor influencing structural safety assessment is the inherent random nature of environmental loads, such as earthquake ground motion, sea waves or gusty winds (see e.g., [36]-[39]). Studies relying on the traditional probabilistic uncertainty model have shown that reliability analysis becomes quite challenging when uncertainties affecting geometrical and/or mechanical properties and the random

nature of excitations are simultaneously taken into account (see e.g., [39]-[41]). From a computational viewpoint, the main difficulty lies in the need to consider two nested loops on the uncertain parameters and random excitation.

To the best of the authors' knowledge, in literature only a few studies have focused on reliability analysis of structures subjected to random excitation with uncertain structural parameters described using non-traditional models. Among these, the most popular approach is the interval model which describes the uncertain parameters as interval variables with given lower bound and upper bound [9],[10], while no information on the probability of occurrence between such bounds is given. Under this assumption, the statistics of structural response in the presence of random excitation have an interval nature and the measure of structural performance is provided by a lower and upper value of reliability or failure probability, rather than by a single value. To estimate the range of the interval reliability, all possible combinations arising between the lower bound and upper bound of the uncertain parameters need to be explored for any sample of the random excitation. This approach requires tremendous computational effort and proves to be unfeasible for real engineering problems with a large number of degrees-of-freedom and uncertain parameters. It follows that efficient procedures able to predict the influence of both random excitations and interval parameters on structural safety need to be developed. In this context, the dynamic response and reliability of truss systems with fuzzy-random parameters under stationary stochastic excitation have been analyzed by Ma et al. [42] by applying a novel two-factor method. An improved particle swarm optimization algorithm for evaluating the range of dynamic reliability of structures with interval design parameters and interval safe bounds under stationary random excitation has been proposed by Do et al. [43]. Muscolino et al. [44]-[46] addressed the reliability analysis of linear discretized structures with interval stiffness properties subjected to stationary Gaussian random excitation by interval extension of the formulation of the *first-passage* problem, under the Poisson assumption of independent up-crossings of a prescribed threshold [36],[38]. As a result of interval uncertainties,

the *cumulative distribution function* (*CDF*) of the *extreme value* response process, also called *reliability function*, is described by an interval function which depends on the interval mean-value and interval spectral moments of zero- and second-order of the selected stationary random response process. In this context, the aim of reliability analysis is the evaluation of the lower bound and upper bound of the *interval reliability function* which define a probability-box (p-box) [47] representative of the range of structural performance under prescribed variations of the uncertain parameters within their respective intervals. By applying the so-called *Interval Rational Series Expansion* (*IRSE*) [48], first an approach based on *first-order interval Taylor series expansion* [44] has been proposed, later on, approximate explicit bounds of the *interval reliability function* [45] and of the *interval fractile* of order *p* [46] have been derived by considering suitable combinations of the endpoints of the interval mean-value and spectral moments of zero- and second-order of the response process. In both cases, interval uncertainties have been described by means of the *Improved Interval Analysis via Extra Unitary Interval* (*IIA* via *EUI*) [49] in order to limit conservatism affecting computations based on the *Classical Interval Analysis* (*CIA*) [9],[10]. Such conservatism is caused by the so-called *dependency phenomenon* which is related to the inability of the *CIA* to treat multiple occurrences of the same interval variables in a mathematical expression as dependent ones. Furthermore, in Ref. [44]-[46] structural failure has been assumed to occur when a displacement component firstly exceeds a critical value. Assuming a selected stress process as the response measure responsible of structural failure is much more challenging due to the high overestimation of the range of stress-related interval functions which typically affects structural analysis based on the rules of the *CIA*. Indeed, stresses are more sensitive to the *dependency phenomenon* than displacements since their expression involves multiple occurrences of the same interval variables. Recently, this issue has been successfully addressed by Sofi et al. [50] who proposed a sensitivity-based procedure for estimating the bounds of the *interval reliability function* for structures with interval axial stiffness assuming the axial stress at a critical location as responsible of structural failure. Recent efforts in literature have been devoted to the solution of the

interval *first-passage* problem taking into account epistemic uncertainties in the stochastic loading model [51],[52].

The main purpose of the present study is the extension of the sensitivity-based procedure proposed by Sofi et al. [50] to general finite element models involving both mass and stiffness uncertainties subjected to stationary Gaussian multi-correlated random excitation with deterministic parameters. The formulation is developed in the context of the *first-passage* theory, under the Poisson assumption of independent up-crossings of a prescribed threshold [36],[38]. It is assumed that the structure fails as soon as a selected stress process at a critical location firstly exceeds a prescribed safe domain. The issue of overestimation is tackled by describing interval uncertainties affecting the mass and stiffness matrices of the structure through the *IIA* via *EUI* [49]. The key idea of the sensitivity-based approach is to examine the sign of sensitivities of the *interval reliability function* with respect to the uncertain parameters in order to identify suitable combinations of the endpoints of interval uncertainties which yield accurate estimates of its bounds as long as monotonic problems are dealt with. Thus, the lower bound and upper bound of the *interval reliability function* are evaluated by performing two stochastic analyses of the randomly excited structure one for each of the two sets of uncertain parameters identified by sensitivity analysis. The same approach is applied to estimate the bounds of the *interval fractile* of order *p* of the selected stress process. The knowledge of sensitivities of the *interval reliability function* is also exploited to analyze the relative importance of the uncertain parameters on structural performance. To enhance the computational efficiency, only the most influential uncertain parameters can be conveniently modeled as interval variables while the remaining parameters can be set to their nominal values.

For validation purpose, a steel telecommunication antenna mast and a ten-story shear-type frame under wind excitation are selected as case-studies.

The rest of the paper is organized as follows. In Section 2, first some basic notions on the interval model of uncertainty [9], [10], with special focus on the *IIA via EUI* [49], are given, then

the problem formulation is presented. Sections 3 and 4 outline the evaluation of the bounds of the *interval reliability function* and of the *interval fractile* of order *p* of the selected stress process by means of the proposed sensitivity-based procedure. In Section 5, two numerical examples are presented to assess the effectiveness of the presented method.

## 2. PROBLEM FORMULATION

### 2.1 Interval model of uncertainty

The interval model may be viewed as the most popular among non-probabilistic approaches for representing uncertainties occurring in engineering problems. The key idea is to describe the $i-\text{th}$ uncertain parameter as an interval variable $\alpha_i^I = \left[\underline{\alpha}_i, \overline{\alpha}_i\right] \in \mathbb{IR}$ [9],[10], where the apex *I* denotes interval variables; $\mathbb{IR}$ indicates the set of all closed real interval numbers, while $\underline{\alpha}_i$ and $\overline{\alpha}_i$ are the *lower bound* (*LB*) and *upper bound* (*UB*) of $\alpha_i^I$, respectively. No information on the likelihood of occurrence of parameter values between the *LB* and *UB* is provided. The $i-\text{th}$ real interval variable $\alpha_i^I$, also referred to as uncertain-but-bounded, is characterized by the midpoint value and the deviation amplitude, defined, respectively, as [9],[10]:

$$\alpha_{0i} = \frac{\underline{\alpha}_i + \overline{\alpha}_i}{2}; \qquad \Delta\alpha_i = \frac{\overline{\alpha}_i - \underline{\alpha}_i}{2}. \tag{1a,b}$$

The main drawback of the *Classical Interval Analysis* (*CIA)* [9],[10] lies in the overestimation of the interval solution range caused by the so-called *dependency phenomenon* which arises when the same interval variable occurs more than once in a mathematical expression. To reduce conservatism in the framework of interval structural analysis, the so-called *Improved Interval Analysis* (*IIA*) via *Extra Unitary Interval* (*EUI*) has been proposed by Muscolino and Sofi [49]. According to this approach, the $i-\text{th}$ interval variable $\alpha_i^I$ is expressed in the following *affine form*:

$$\alpha_i^I = \alpha_{0i} + \Delta\alpha_i \hat{e}_i^I \tag{2}$$

where $\hat{e}_i^I \triangleq [-1,+1]$ is a particular unitary interval, called *EUI*, which does not obey the rules of the *CIA*. An *EUI* is associated with each interval variable, so that uncertainties can be traced throughout computations. If $\alpha_i^I$ is a symmetric interval variable, Eq. (2) reduces to $\alpha_i^I = \Delta\alpha_i \hat{e}_i^I$ since $\underline{\alpha}_i = -\overline{\alpha}_i$ and, therefore, $\alpha_{0i} = 0$.

In the framework of interval symbolism, a generic interval-valued function $f$ and a generic interval-valued matrix function $\mathbf{A}$ of the interval vector $\boldsymbol{\alpha}^I$ will be denoted in equivalent form, respectively, as:

$$\begin{aligned} f^I &\equiv f(\boldsymbol{\alpha}^I) \Leftrightarrow f(\boldsymbol{\alpha}), \quad \boldsymbol{\alpha} \in \boldsymbol{\alpha}^I = \left[\underline{\boldsymbol{\alpha}}, \overline{\boldsymbol{\alpha}}\right]; \\ \mathbf{A}^I &\equiv \mathbf{A}(\boldsymbol{\alpha}^I) \Leftrightarrow \mathbf{A}(\boldsymbol{\alpha}), \quad \boldsymbol{\alpha} \in \boldsymbol{\alpha}^I = \left[\underline{\boldsymbol{\alpha}}, \overline{\boldsymbol{\alpha}}\right]. \end{aligned} \tag{3a,b}$$

## 2.2 Equations of motion

Let us consider a linear-elastic structure subjected to a stationary Gaussian multi-correlated stochastic process $\mathbf{F}(t)$. The structure is discretized into $N^{(e)}$ finite elements (FEs) resulting into a $n$-DOFs model. Young's modulus and mass density of the $i$-th FE are assumed uncertain and are described as interval variables by means of the *IIA* via *EUI* [49], i.e.

$$E^{(i)}(\alpha_{(\mathrm{K})i}^I) = E_0^{(i)}\left(1 + \alpha_{(\mathrm{K})i}^I\right) = E_0^{(i)}\left(1 + \Delta\alpha_{(\mathrm{K})i}\hat{e}_{(\mathrm{K})i}^I\right), \quad i = 1,2,\ldots,r_{\mathrm{K}} \tag{4}$$

and

$$\rho^{(i)}(\alpha_{(\mathrm{M})i}^I) = \rho_0^{(i)}\left(1 + \alpha_{(\mathrm{M})i}^I\right) = \rho_0^{(i)}\left(1 + \Delta\alpha_{(\mathrm{M})i}\hat{e}_{(\mathrm{M})i}^I\right), \quad i = 1,2,\ldots,r_{\mathrm{M}} \tag{5}$$

where the subscripts K and M mean that the uncertain Young's moduli and mass densities affect the stiffness and mass matrices of the structure; $r_{\mathrm{K}} \le N^{(e)}$ and $r_{\mathrm{M}} \le N^{(e)}$ denote the number of FEs with uncertain stiffness and mass matrix, respectively; $\alpha_{(\mathrm{K})i}^I$ and $\alpha_{(\mathrm{M})i}^I$ are symmetric interval variables denoting the dimensionless fluctuations of Young's modulus and mass density around the nominal values $E_0^{(i)}$ and $\rho_0^{(i)}$, respectively; $\Delta\alpha_{(\mathrm{K})i}$, $\Delta\alpha_{(\mathrm{M})i}$ and $\hat{e}_{(\mathrm{K})i}^I$, $\hat{e}_{(\mathrm{M})i}^I$ represent the associated

deviation amplitudes and *EUI*s. It is assumed that the fluctuations $\alpha^I_{(\mathrm{K})i}$ and $\alpha^I_{(\mathrm{M})i}$ vary independently.

Taking into account Eq.(4), the elastic matrix of the $i$-th FE can be expressed as:

$$\mathbf{E}^{(i)}(\alpha^I_{(\mathrm{K})i}) = \left(1 + \Delta\alpha_{(\mathrm{K})i}\hat{e}^I_{(\mathrm{K})i}\right)\mathbf{E}^{(i)}_0 \tag{6}$$

where $\mathbf{E}^{(i)}_0$ is the element elastic matrix with nominal Young's modulus $E^{(i)}_0$.

Let $\boldsymbol{\alpha}^I \in \mathbb{IR}^r$ be a bounded interval vector, defined as

$$\boldsymbol{\alpha}^I = \left[\underline{\boldsymbol{\alpha}}, \overline{\boldsymbol{\alpha}}\right] = \left[\left(\boldsymbol{\alpha}^I_{\mathrm{K}}\right)^{\mathrm{T}} \quad \left(\boldsymbol{\alpha}^I_{\mathrm{M}}\right)^{\mathrm{T}}\right]^{\mathrm{T}} \tag{7}$$

where the apex T denotes the transpose matrix operator; $\boldsymbol{\alpha}^I_{\mathrm{K}} \in \mathbb{IR}^{r_{\mathrm{K}}}$ and $\boldsymbol{\alpha}^I_{\mathrm{M}} \in \mathbb{IR}^{r_{\mathrm{M}}}$ are interval vectors collecting the fluctuations $\alpha^I_{(\mathrm{K})i}$ and $\alpha^I_{(\mathrm{M})i}$, such that $\alpha^I_i = \alpha^I_{(\mathrm{K})i}$ if $i \le r_{\mathrm{K}}$ and $\alpha^I_i = \alpha^I_{(\mathrm{M})i}$ if $i > r_{\mathrm{K}}$, with $r = r_{\mathrm{K}} + r_{\mathrm{M}}$ being the total number of uncertain parameters; the symbols $\underline{\boldsymbol{\alpha}}$ and $\overline{\boldsymbol{\alpha}}$ denote the vectors gathering the *LB* and *UB* of the interval parameters $\alpha^I_i$ $(i = 1,2,\ldots,r = r_{\mathrm{K}} + r_{\mathrm{M}})$, respectively, such that $\underline{\boldsymbol{\alpha}} \le \boldsymbol{\alpha} \le \overline{\boldsymbol{\alpha}}$. The midpoint values and the deviation amplitudes of $\alpha^I_i$, $\alpha_{0i}$ and $\Delta\alpha_i$, are collected into the vectors $\boldsymbol{\alpha}_0$ and $\Delta\boldsymbol{\alpha}$, respectively. For the sake of simplicity, it is assumed that $r_{\mathrm{K}} = r_{\mathrm{M}} = N^{(e)}$, so that the number of uncertain parameters is $r = r_{\mathrm{K}} + r_{\mathrm{M}} = 2N^{(e)}$.

It is worth mentioning that uncertain material properties generally exhibit a spatial variability which requires a suitable mathematical representation. To this aim, within the interval framework, the interval field model has been developed [53]. This model describes spatially dependent properties as a superposition of suitable basis functions representing the spatial character, weighted by independent interval coefficients accounting for uncertainty. The interval field description of an uncertain property can be incorporated into the standard FEM by applying a suitable discretization procedure, which reduces the spatially dependent property to a set of independent interval variables [54]. This entails that the present formulation can be readily extended to the case of uncertain properties modelled as interval fields.

Let $\mathbf{x} = [x_1 \quad x_2 \quad x_3]^{\mathrm{T}}$ indicate the position vector of a generic point referred to a Cartesian coordinate system $O(x_1, x_2, x_3)$. Following the standard displacement-based FE formulation, the interval displacement field within the $i$-th FE can be approximated as follows:

$$\mathbf{u}^{(i)}(\boldsymbol{\alpha}^I, \mathbf{x}, t) = \mathbf{N}^{(i)}(\mathbf{x})\mathbf{d}^{(i)}(\boldsymbol{\alpha}^I, t) \tag{8}$$

where $\mathbf{N}^{(i)}(\mathbf{x})$ denotes the shape-function matrix; $\mathbf{d}^{(i)}(\boldsymbol{\alpha}^I, t)$ is the nodal displacement vector of the $i$-th FE depending both on time $t$ and on the interval fluctuations collected into the vector $\boldsymbol{\alpha}^I$ (see Eq. (7)).

The strain-displacement equations and the linear-elastic constitutive equations yield the following expressions of the interval strain and stress fields within the $i$-th FE:

$$\boldsymbol{\varepsilon}^{(i)}(\boldsymbol{\alpha}^I, \mathbf{x}, t) = \mathbf{B}^{(i)}(\mathbf{x})\mathbf{d}^{(i)}(\boldsymbol{\alpha}^I, t) \tag{9}$$

and

$$\boldsymbol{\sigma}^{(i)}(\boldsymbol{\alpha}^I, \mathbf{x}, t) = \mathbf{E}^{(i)}(\alpha^I_{(\mathrm{K})i})\boldsymbol{\varepsilon}^{(i)}(\boldsymbol{\alpha}^I, \mathbf{x}, t) = \left(1 + \Delta\alpha_{(\mathrm{K})i}\hat{e}^I_{(\mathrm{K})i}\right)\mathbf{E}_0^{(i)}\mathbf{B}^{(i)}(\mathbf{x})\mathbf{d}^{(i)}(\boldsymbol{\alpha}^I, t) \tag{10}$$

where $\mathbf{B}^{(i)}(\mathbf{x})$ is the strain-displacement matrix and the definition of the interval elastic matrix $\mathbf{E}^{(i)}(\alpha^I_{(\mathrm{K})i})$ in Eq. (6) has been taken into account.

The stiffness matrix of the $i$-th FE is an interval matrix, formally analogous to the one pertaining to the deterministic FE, i.e.:

$$\mathbf{k}^{(i)}(\alpha^I_{(\mathrm{K})i}) = \int_{V^{(i)}} \mathbf{B}^{(i)\mathrm{T}}(\mathbf{x})\mathbf{E}^{(i)}(\alpha^I_{(\mathrm{K})i})\mathbf{B}^{(i)}(\mathbf{x})\mathrm{d}V^{(i)} = \left(1 + \Delta\alpha_{(\mathrm{K})i}\hat{e}^I_{(\mathrm{K})i}\right)\mathbf{k}_0^{(i)} \tag{11}$$

where $V^{(i)}$ is the volume of the $i$-th FE; $\mathbf{k}_0^{(i)} = \mathbf{k}^{(i)}(\alpha_{(\mathrm{K})i})\big|_{\alpha_{(\mathrm{K})i}=0}$ is the nominal element stiffness matrix and $\mathbf{E}^{(i)}(\alpha^I_{(\mathrm{K})i})$ is the interval elastic matrix given by Eq. (6).

The mass matrix of the $i$-th FE is an interval matrix as well, defined as:

$$\mathbf{m}^{(i)}(\alpha^I_{(\mathrm{M})i}) = \int_{V^{(i)}} \rho^{(i)}(\alpha^I_{(\mathrm{M})i})\mathbf{N}^{(i)\mathrm{T}}(\mathbf{x})\mathbf{N}^{(i)}(\mathbf{x})\mathrm{d}V^{(i)} = \left(1 + \Delta\alpha_{(\mathrm{M})i}\hat{e}^I_{(\mathrm{M})i}\right)\mathbf{m}_0^{(i)} \tag{12}$$

where $\mathbf{m}_0^{(i)} = \mathbf{m}^{(i)}(\alpha_{(\mathrm{M})i})\big|_{\alpha_{(\mathrm{M})i}=0}$ is the nominal element mass matrix.

Notice that the interval stiffness and mass matrices of the $i$-th FE in Eqs. (11) and (12) depend only on the $i$-th uncertain Young's modulus and mass density, respectively, through the associated *EUI*s. Such a feature plays a crucial role in order to reduce overestimation in the context of interval FE analysis since the generic uncertain physical property is linked to the pertinent FE by means of the associated *EUI*. This allows us to treat multiple occurrences of the same interval variable as dependent ones both in the assembly and solution phases of interval FE analysis [55].

The nodal displacement vector of the $i$-th FE, $\mathbf{d}^{(i)}(\boldsymbol{\alpha}^I,t)$, can be related to the global nodal displacements collected into the interval vector $\mathbf{U}(\boldsymbol{\alpha}^I,t)$ as:

$$\mathbf{d}^{(i)}(\boldsymbol{\alpha}^I,t)=\mathbf{L}^{(i)}\mathbf{U}(\boldsymbol{\alpha}^I,t) \tag{13}$$

where $\mathbf{L}^{(i)}$ is a Boolean matrix defined so as to take into account the boundary conditions. Then, assuming for the sake of simplicity that all the quantities are referred to the global coordinate system, the standard assembly procedure yields the following interval global equations of motion:

$$\mathbf{M}^I\ddot{\mathbf{U}}^I(t)+\mathbf{C}^I\dot{\mathbf{U}}^I(t)+\mathbf{K}^I\mathbf{U}^I(t)=\mathbf{F}(t) \tag{14}$$

where $\mathbf{U}^I(t)\equiv\mathbf{U}(\boldsymbol{\alpha}^I,t)$ is the interval stationary Gaussian vector process of global nodal displacements; a dot over a variable denotes differentiation with respect to time $t$; $\mathbf{K}^I$ and $\mathbf{M}^I$ are the interval global stiffness and mass matrices, defined as:

$$\mathbf{K}^I\equiv\mathbf{K}(\boldsymbol{\alpha}_{\mathrm{K}}^I)=\mathbf{K}_0+\sum_{i=1}^{r_{\mathrm{K}}}\mathbf{K}_i\Delta\alpha_{(\mathrm{K})i}\hat{e}^I_{(\mathrm{K})i} \tag{15}$$

and

$$\mathbf{M}^I\equiv\mathbf{M}(\boldsymbol{\alpha}_{\mathrm{M}}^I)=\mathbf{M}_0+\sum_{i=1}^{r_{\mathrm{M}}}\mathbf{M}_i\Delta\alpha_{(\mathrm{M})i}\hat{e}^I_{(\mathrm{M})i} \tag{16}$$

where $\mathbf{K}_0=\mathbf{K}(\boldsymbol{\alpha}_{\mathrm{K}})\big|_{\boldsymbol{\alpha}_{\mathrm{K}}=\mathbf{0}}$ and $\mathbf{M}_0=\mathbf{M}(\boldsymbol{\alpha}_{\mathrm{M}})\big|_{\boldsymbol{\alpha}_{\mathrm{M}}=\mathbf{0}}$ are the nominal global stiffness and mass matrices, respectively; and the matrices $\mathbf{K}_i$ and $\mathbf{M}_i$ are given by:

$$\mathbf{K}_i = \left.\frac{\partial \mathbf{K}(\boldsymbol{\alpha}_{\mathrm{K}}^I)}{\partial \alpha_{(\mathrm{K})i}}\right|_{\boldsymbol{\alpha}_{\mathrm{K}}=\mathbf{0}} = \mathbf{L}^{(i)\mathrm{T}}\mathbf{k}_0^{(i)}\mathbf{L}^{(i)}; \qquad \mathbf{M}_i = \left.\frac{\partial \mathbf{M}(\boldsymbol{\alpha}_{\mathrm{M}}^I)}{\partial \alpha_{(\mathrm{M})i}}\right|_{\boldsymbol{\alpha}_{\mathrm{M}}=\mathbf{0}} = \mathbf{L}^{(i)\mathrm{T}}\mathbf{m}_0^{(i)}\mathbf{L}^{(i)}. \qquad (17a,b)$$

Notice that both the interval matrices in Eqs. (15) and (16) are expressed as sum of the nominal value plus an interval deviation given by the superposition of the contributions of the pertinent uncertain parameters which are identified by the associated *EUI*s.

By adopting the Rayleigh model, the global damping matrix $\mathbf{C}^I$ turns out to be an interval matrix as well, defined as:

$$\mathbf{C}^I \equiv \mathbf{C}(\boldsymbol{\alpha}^I) = c_0\mathbf{M}^I + c_1\mathbf{K}^I = \mathbf{C}_0 + c_0\sum_{i=1}^{r_{\mathrm{M}}}\mathbf{M}_i\Delta\alpha_{(\mathrm{M})i}\hat{e}^I_{(\mathrm{M})i} + c_1\sum_{i=1}^{r_{\mathrm{K}}}\mathbf{K}_i\Delta\alpha_{(\mathrm{K})i}\hat{e}^I_{(\mathrm{K})i} \qquad (18)$$

where $\mathbf{C}_0 = c_0\mathbf{M}_0 + c_1\mathbf{K}_0$ is the nominal damping matrix; $c_0$ and $c_1$ denote the Rayleigh damping constants, herein evaluated setting the uncertain parameters equal to their nominal values.

As customary, the external load vector $\mathbf{F}(t)$ in Eq. (14) can be expressed as sum of the mean-value $\boldsymbol{\mu}_{\mathbf{F}}=\mathrm{E}\langle\mathbf{F}(t)\rangle$, with $\mathrm{E}\langle\bullet\rangle$ denoting the stochastic average operator, plus a zero-mean random fluctuating component $\tilde{\mathbf{X}}_{\mathbf{F}}(t)$, i.e. $\mathbf{F}(t) = \boldsymbol{\mu}_{\mathbf{F}} + \tilde{\mathbf{X}}_{\mathbf{F}}(t)$. Thus, in the frequency domain, the full probabilistic characterization of the external load vector $\mathbf{F}(t)$ requires the knowledge of the mean-value vector, $\boldsymbol{\mu}_{\mathbf{F}}=\mathrm{E}\langle\mathbf{F}(t)\rangle$, and of the one-sided *Power Spectral Density* (*PSD*) function matrix $\mathbf{G}_{\tilde{\mathbf{X}}_{\mathbf{F}}\tilde{\mathbf{X}}_{\mathbf{F}}}(\omega)$ of the fluctuating component $\tilde{\mathbf{X}}_{\mathbf{F}}(t)$.

### 2.3 Interval stationary Gaussian stochastic response process

The interval stationary Gaussian stochastic response process $\mathbf{U}^I(t)$, ruled by the equations of motion in Eq.(14), is completely characterized in the frequency domain by the interval mean-value vector:

$$\boldsymbol{\mu}_{\mathbf{U}}^I \equiv \boldsymbol{\mu}_{\mathbf{U}}(\boldsymbol{\alpha}_{\mathrm{K}}^I) = \mathrm{E}\left\langle\mathbf{U}^I(t)\right\rangle = \mathbf{K}^{-1}(\boldsymbol{\alpha}_{\mathrm{K}}^I)\boldsymbol{\mu}_{\mathbf{F}} \qquad (19)$$

and by the interval one-sided *PSD* function matrix, $\mathbf{G}^I_{\mathbf{UU}}(\omega) \equiv \mathbf{G}_{\mathbf{UU}}(\boldsymbol{\alpha}^I,\omega)$, defined as follows:

$$\mathbf{G}^I_{\mathbf{UU}}(\omega) \equiv \mathbf{G}_{\mathbf{UU}}(\boldsymbol{\alpha}^I,\omega) = \mathbf{H}^*(\boldsymbol{\alpha}^I,\omega)\mathbf{G}_{\tilde{\mathbf{X}}_{\mathbf{F}}\tilde{\mathbf{X}}_{\mathbf{F}}}(\omega)\mathbf{H}^{\mathrm{T}}(\boldsymbol{\alpha}^I,\omega) \qquad (20)$$

where the asterisk means complex conjugate, and $\mathbf{H}(\boldsymbol{\alpha}^I,\omega)$ is the interval *Frequency Response Function* (*FRF*) matrix, or *Transfer Function* matrix, given by:

$$\mathbf{H}^I(\omega)\equiv\mathbf{H}(\boldsymbol{\alpha}^I,\omega)=\left[-\omega^2\mathbf{M}^I+\mathrm{j}\omega\mathbf{C}^I+\mathbf{K}^I\right]^{-1} \tag{21}$$

with $\mathrm{j}=\sqrt{-1}$ denoting the imaginary unit.

The generic response quantity of interest (e.g., displacement, strain or stress at a critical point), can be determined from the knowledge of the vector $\mathbf{U}^I(t)\equiv\mathbf{U}(\boldsymbol{\alpha}^I,t)$ of global nodal displacements.

Attention is herein focused on the $j$-th component of the interval stationary Gaussian random stress vector process $\boldsymbol{\sigma}^{(h)}(\boldsymbol{\alpha}^I,\mathbf{x},t)$ (see Eq. (10)) at a given position $\mathbf{x}$ within the $h$-th FE:

$$Y_j^{(h)I}(t)\equiv\sigma_j^{(h)}(\boldsymbol{\alpha}^I,\mathbf{x},t)=\left(1+\Delta\alpha_{(\mathrm{K})h}\hat{e}^I_{(\mathrm{K})h}\right)\mathbf{r}_j^{(h)\mathrm{T}}(\mathbf{x})\mathbf{U}(\boldsymbol{\alpha}^I,t) \tag{22}$$

where $\mathbf{r}_j^{(h)\mathrm{T}}(\mathbf{x})$ is the $j$-th row of the $n\times n$ matrix

$$\mathbf{R}^{(h)}(\mathbf{x})=\mathbf{E}_0^{(h)}\mathbf{B}^{(h)}(\mathbf{x})\mathbf{L}^{(h)}. \tag{23}$$

To simplify the notation, the dependence of $\mathbf{r}_j^{(h)}$ on $\mathbf{x}$ is hereinafter omitted since the stress is evaluated at a given position.

By inspection of Eq.(22), it is readily inferred that the interval variable $\alpha^I_{(\mathrm{K})h}=\Delta\alpha_{(\mathrm{K})h}\hat{e}^I_{(\mathrm{K})h}$ occurs more than once. It follows that quantities related to interval stresses are more vulnerable to the *dependency phenomenon* than displacements.

The interval stationary Gaussian stress random process in Eq.(22) can be expressed as sum of the interval mean-value value, $\mu^I_{Y_j^{(h)}}$, plus a zero-mean random fluctuation, $\tilde{Y}_j^{(h)I}(t)$, i.e. $Y_j^{(h)I}(t)=\mu^I_{Y_j^{(h)}}+\tilde{Y}_j^{(h)I}(t)$. Its complete probabilistic characterization in the frequency domain thus requires the knowledge of the interval mean-value, $\mu^I_{Y_j^{(h)}}$, and of the interval one-sided *PSD* function, $G^I_{\tilde{Y}_j^{(h)}\tilde{Y}_j^{(h)}}(\omega)\equiv G^I_{Y_j^{(h)}Y_j^{(h)}}(\omega)$, of the zero-mean random fluctuation process $\tilde{Y}_j^{(h)I}(t)$. The

interval mean-value $\mu^I_{Y_j^{(h)}}$ can be evaluated by applying the stochastic average operator to both sides of Eq.(22), i.e.:

$$\mu^I_{Y_j^{(h)}} \equiv \mu_{Y_j^{(h)}}(\boldsymbol{\alpha}^I_{\mathrm{K}}) = \mathrm{E}\left\langle Y_j^{(h)I}(t)\right\rangle = \left(1+\Delta\alpha_{(\mathrm{K})h}\hat{e}^I_{(\mathrm{K})h}\right)\mathbf{r}_j^{(h)\mathrm{T}}\boldsymbol{\mu}_{\mathbf{U}}(\boldsymbol{\alpha}^I_{\mathrm{K}}) \tag{24}$$

where $\boldsymbol{\mu}_{\mathbf{U}}(\boldsymbol{\alpha}^I_{\mathrm{K}})$ is the interval mean-value of the displacement vector given in Eq. (19), which obviously does not depend on the fluctuations $\boldsymbol{\alpha}^I_{\mathrm{M}}$ of the uncertain mass densities.

Based on Eqs. (20) and (22), the interval one-sided *PSD* function $G^I_{\tilde{Y}_j^{(h)}\tilde{Y}_j^{(h)}}(\omega) \equiv G^I_{Y_j^{(h)}Y_j^{(h)}}(\omega)$ of the interval stress random process $Y_j^{(h)I}(t)$ takes the following form:

$$G^I_{Y_j^{(h)}Y_j^{(h)}}(\omega) \equiv G_{Y_j^{(h)}Y_j^{(h)}}(\boldsymbol{\alpha}^I,\omega) = \left(1+\Delta\alpha_{(\mathrm{K})h}\hat{e}^I_{(\mathrm{K})h}\right)^2 \mathbf{r}_j^{(h)\mathrm{T}}\,\mathbf{H}^*(\boldsymbol{\alpha}^I,\omega)\mathbf{G}_{\tilde{\mathbf{X}}_{\mathbf{F}}\tilde{\mathbf{X}}_{\mathbf{F}}}(\omega)\mathbf{H}^{\mathrm{T}}(\boldsymbol{\alpha}^I,\omega)\mathbf{r}_j^{(h)}. \tag{25}$$

Notice that the same interval variables occur more than once in the previous equation. This implies that the statistics of the interval stress random process may be affected by serious overestimation due to the *dependency phenomenon*.

## 3. BOUNDS OF THE INTERVAL RELIABILITY FUNCTION

### 3.1 Interval reliability function

Failure or unsatisfactory performance of a structural system is herein identified with the *first-passage failure* which occurs when the *extreme value* random process for some response measure (e.g., displacement, strain or stress) firstly exceeds a prescribed safe domain within a specified time interval $[0,T]$. Specifically, it is assumed that the structure fails in a *first-passage* sense if the $j$-th component of the interval stationary Gaussian random stress vector process $\boldsymbol{\sigma}^{(h)}(\boldsymbol{\alpha}^I,\mathbf{x},t)$ (see Eq. (10)) at a given position $\mathbf{x}$ within the $h$-th FE, i.e. $Y_j^{(h)}(\boldsymbol{\alpha}^I,t)$ (see Eq. (22)), reaches a prescribed threshold.

The *extreme value* random process of $Y_j^{(h)}(\boldsymbol{\alpha}^I,t)$, over the time interval $[0,T]$, has an interval

nature and is mathematically defined as:

$$Y_{j,\max}^{(h)I}(T) \equiv Y_{j,\max}^{(h)}(\boldsymbol{\alpha}^I, T) = \max_{0 \le t \le T} \left| Y_j^{(h)}(\boldsymbol{\alpha}^I, t) \right| \tag{26}$$

where the symbol $|\bullet|$ denotes absolute value.

The probability that $Y_{j,\max}^{(h)}(\boldsymbol{\alpha}^I, T)$ is equal to or less than the critical level $b > 0$ within the time interval $[0,T]$ is defined by the *cumulative distribution function* (*CDF*), also called *reliability function*, which has an interval nature as well:

$$L_{Y_{j,\max}^{(h)}}^{I}(b,T) \equiv L_{Y_{j,\max}^{(h)}}(\boldsymbol{\alpha}^I, b, T) = \Pr\left[ Y_{j,\max}^{(h)}(\boldsymbol{\alpha}^I, T) \le b \right] = \left[ \underline{L}_{Y_{j,\max}^{(h)}}(b,T), \quad \overline{L}_{Y_{j,\max}^{(h)}}(b,T) \right]. \tag{27}$$

The *LB* (or right bound) and *UB* (or left bound) of the interval *CDF* define a probability box (p-box) [47] representative of the range of structural performance under prescribed variations of the uncertain parameters within their respective intervals.

For stochastic processes having mean-value different from zero, it is known that the *interval CDF*, $L_{Y_{j,\max}^{(h)}}(\boldsymbol{\alpha}^I, b, T)$, of the *extreme value* random process $Y_{j,\max}^{(h)}(\boldsymbol{\alpha}^I, T)$ formally coincides with the *interval CDF* of the *extreme value* random process $\tilde{Y}_{j,\max}^{(h)}(\boldsymbol{\alpha}^I, T) = \max_{0 \le t \le T} \left| \tilde{Y}_j^{(h)}(\boldsymbol{\alpha}^I, t) \right| = Y_{j,\max}^{(h)}(\boldsymbol{\alpha}^I, T) - \left| \boldsymbol{\mu}_{Y_j^{(h)}}(\boldsymbol{\alpha}^I) \right|$, where $\tilde{Y}_j^{(h)}(\boldsymbol{\alpha}^I, t)$ denotes the zero-mean interval stationary stochastic process describing the random fluctuation of $Y_j^{(h)}(\boldsymbol{\alpha}^I, t)$ around the interval mean-value $\mu_{Y_j^{(h)}}^I$ (see e.g., [56]).

If the Poisson assumption of independent up-crossings of a prescribed threshold is applied, then the *interval CDF* for unit initial probability can be expressed as (see e.g., [36]):

$$L_{Y_{j,\max}^{(h)}}^{I}(b,T) = \Pr\left[ Y_{j,\max}^{(h)}(\boldsymbol{\alpha}^I, T) \le b \right] \approx \exp\left\{ -T \, \nu_{Y_j^{(h)}}^{+}(\boldsymbol{\alpha}^I) \exp\left[ -\frac{\left( b - \left| \mu_{Y_j^{(h)}}(\boldsymbol{\alpha}^I) \right| \right)^2}{2\lambda_{0,Y_j^{(h)}}(\boldsymbol{\alpha}^I)} \right] \right\} \tag{28}$$

where

$$\nu^{+}_{Y_j^{(h)}}(\boldsymbol{\alpha}^I) = \frac{1}{2\pi}\sqrt{\frac{\lambda_{2,Y_j^{(h)}}(\boldsymbol{\alpha}^I)}{\lambda_{0,Y_j^{(h)}}(\boldsymbol{\alpha}^I)}} \tag{29}$$

is the mean up-crossing rate at level $\left|\mu_{Y_j^{(h)}}(\boldsymbol{\alpha}^I)\right|$; $\lambda_{0,Y_j^{(h)}}(\boldsymbol{\alpha}^I)$ and $\lambda_{2,Y_j^{(h)}}(\boldsymbol{\alpha}^I)$ are the interval spectral moments of zero- and second-order, respectively, of the interval stress random process, $Y_j^{(h)I}(t)$, given by

$$\lambda_{\ell,Y_j^{(h)}}(\boldsymbol{\alpha}^I) = \int_0^\infty \omega^\ell \; G_{Y_j^{(h)}Y_j^{(h)}}(\boldsymbol{\alpha}^I,\omega)\,\mathrm{d}\omega, \quad (\ell = 0, 2) \tag{30}$$

where $G_{Y_j^{(h)}Y_j^{(h)}}(\boldsymbol{\alpha}^I,\omega)$ is the one-sided interval *PSD* function of $Y_j^{(h)I}(t)$ defined in Eq.(25).

Once the *interval CDF* is known, the *interval probability of failure* can be evaluated as follows:

$$P^I_{f,Y^{(h)}_{j,\max}}(b,T) \equiv P_{f,Y^{(h)}_{j,\max}}(\boldsymbol{\alpha}^I, b, T) = \Pr\left[Y^{(h)}_{j,\max}(\boldsymbol{\alpha}^I,T) > b\right] = \left[\underline{P}_{f,Y^{(h)}_{j,\max}}(b,T), \quad \overline{P}_{f,Y^{(h)}_{j,\max}}(b,T)\right] \tag{31}$$

where the *LB* and *UB* are given by:

$$\underline{P}_{f,Y^{(h)}_{j,\max}}(b,T) = 1 - \overline{L}_{Y^{(h)}_{j,\max}}(b,T); \quad \overline{P}_{f,Y^{(h)}_{j,\max}}(b,T) = 1 - \underline{L}_{Y^{(h)}_{j,\max}}(b,T). \tag{32a,b}$$

### 3.2 Proposed sensitivity-based procedure

Reliability analysis of structures with interval parameters under random excitation leads to a range of structural performance rather than providing a crisp value of the reliability or failure probability. In the context of the *first-passage* theory, the aim of reliability analysis is the evaluation of the *LB* and *UB* of the *interval reliability function* defined by Eq. (28). This might be a challenging task when the response measure responsible of structural failure is a stress component at some critical location. Indeed, interval stress-related quantities are more affected by overestimation than displacements. In order to reduce conservatism, which may be detrimental in reliability analysis, the bounds of the *interval reliability function* of the *extreme value* stress random process $Y^{(h)}_{j,\max}(\boldsymbol{\alpha}^I,T)$ are herein evaluated by applying a sensitivity-based procedure. The key idea of this procedure is to

perform a preliminary sensitivity analysis to identify suitable combinations of the endpoints of the interval parameters which provide accurate estimates of the *LB* and *UB* of the *interval CDF* as long as monotonic problems are dealt with.

The chain rule of differentiation yields the following expression of the sensitivity of the *CDF* of the *extreme value* stress random process $Y_{j,\max}^{(h)}(\boldsymbol{\alpha}^I, T)$ with respect to the uncertain parameters $\alpha_i \in \alpha_i^I \ \ (i = 1, 2, \ldots, r)$ [50]:

$$S_{L_{Y_{j,\max}^{(h)}},i}(b,T) = \left.\frac{\partial L_{Y_{j,\max}^{(h)}}(\boldsymbol{\alpha}, b, T)}{\partial \alpha_i}\right|_{\boldsymbol{\alpha}=\mathbf{0}}$$

$$= C_{Y_j^{(h)}}(b,T)\left\{2\left(b - \left|\mu_{Y_j^{(h)}}^{(0)}\right|\right)\frac{\left|\mu_{Y_j^{(h)}}^{(0)}\right|}{\mu_{Y_j^{(h)}}^{(0)}} S_{\mu_{Y_j^{(h)}},i} + \left[\frac{\left(b - \left|\mu_{Y_j^{(h)}}^{(0)}\right|\right)^2}{\lambda_{0,Y_j^{(h)}}^{(0)}} - 1\right] S_{\lambda_{0,Y_j^{(h)}},i} + \frac{\lambda_{0,Y_j^{(h)}}^{(0)}}{\lambda_{2,Y_j^{(h)}}^{(0)}} S_{\lambda_{2,Y_j^{(h)}},i}\right\} \tag{33}$$

where $\mu_{Y_j^{(h)}}^{(0)}$ and $\lambda_{\ell,Y_j^{(h)}}^{(0)}$ $(\ell = 0, 2)$ denote the nominal mean-value and spectral moments of the selected stress process, given by Eqs. (24) and (30) with $\boldsymbol{\alpha} = \mathbf{0}$; the function $C_{Y_j^{(h)}}(b,T)$ is defined as follows:

$$C_{Y_j^{(h)}}(b,T) = -\frac{T}{4\pi}\frac{\lambda_{2,Y_j^{(h)}}^{(0)}}{\lambda_{0,Y_j^{(h)}}^{(0)}}\frac{L_{Y_{j,\max}^{(h)}}^{(0)}(b,T)}{\sqrt{\lambda_{0,Y_j^{(h)}}^{(0)}\ \lambda_{2,Y_j^{(h)}}^{(0)}}}\exp\left[-\frac{\left(b - \left|\mu_{Y_j^{(h)}}^{(0)}\right|\right)^2}{2\lambda_{0,Y_j^{(h)}}^{(0)}}\right] \tag{34}$$

with $L_{Y_{j,\max}^{(h)}}^{(0)}(b,T) = \left. L_{Y_{j,\max}^{(h)}}(\boldsymbol{\alpha}, b, T)\right|_{\boldsymbol{\alpha}=\mathbf{0}}$ denoting the nominal *CDF*. Furthermore, in Eq.(33) $S_{\mu_{Y_j^{(h)}},i}$ is the sensitivity of the mean-value $\mu_{Y_j^{(h)}}(\boldsymbol{\alpha}_{\mathrm{K}})$ of the interval stress random process (see Eq. (24)) with respect to the uncertain parameter $\alpha_i = \alpha_{(\mathrm{K})i}$, which can be evaluated as:

$$\text{if} \quad i = h \quad \text{then} \quad S_{\mu_{Y_j^{(h)}},i} = \left.\frac{\partial \mu_{Y_j^{(h)}}(\boldsymbol{\alpha}_{\mathrm{K}})}{\partial \alpha_i}\right|_{\boldsymbol{\alpha}_{\mathrm{K}}=\mathbf{0}} = \mu_{Y_j^{(h)}}^{(0)} - \mathbf{r}_j^{(h)\mathrm{T}}\,\mathbf{K}_0^{-1}\mathbf{K}_h\,\mathbf{K}_0^{-1}\boldsymbol{\mu}_{\mathbf{F}} \tag{35}$$

$$\text{if} \quad i \neq h \quad \text{then} \quad S_{\mu_{Y_j^{(h)}},i} = \left. \frac{\partial \mu_{Y_j^{(h)}}(\boldsymbol{\alpha}_{\mathrm{K}})}{\partial \alpha_i} \right|_{\boldsymbol{\alpha}_{\mathrm{K}}=\mathbf{0}} = -\mathbf{r}_j^{(h)\mathrm{T}} \mathbf{K}_0^{-1} \mathbf{K}_i \mathbf{K}_0^{-1} \boldsymbol{\mu}_{\mathbf{F}} \tag{36}$$

where $\mathbf{K}_0$ is the nominal stiffness matrix; $\mathbf{K}_i$ is given by Eq. (17a); and $\mathbf{K}_0^{-1}\mathbf{K}_i \mathbf{K}_0^{-1}\boldsymbol{\mu}_{\mathbf{F}}$ is the $i-$th sensitivity of $\boldsymbol{\mu}_{\mathbf{U}}(\boldsymbol{\alpha}_{\mathrm{K}})$ (see Eq. (19)).

Finally, in Eq.(33), $S_{\lambda_{\ell,Y_j^{(h)}},i}$ denotes the sensitivity of the spectral moment of order $\ell$ of the interval stress random process $Y_j^{(h)}(\boldsymbol{\alpha}^I, t)$ with respect to the $i-$th parameter $\alpha_i$:

$$S_{\lambda_{\ell,Y_j^{(h)}},i} = \left. \frac{\partial \lambda_{\ell,Y_j^{(h)}}(\boldsymbol{\alpha})}{\partial \alpha_i} \right|_{\boldsymbol{\alpha}=\mathbf{0}} = \int_0^{\infty} \omega^{\ell} S_{G_{Y_j^{(h)}Y_j^{(h)}},i}(\omega)\,\mathrm{d}\omega, \quad (\ell = 0, 2). \tag{37}$$

In the previous expression, $S_{G_{Y_j^{(h)}Y_j^{(h)}},i}(\omega)$ is the $i-$th sensitivity of the one-sided *PSD* function $G_{Y_j^{(h)}Y_j^{(h)}}(\boldsymbol{\alpha}^I, \omega)$ (see Eq. (25)) which has to be evaluated distinguishing the following two cases:

**Case 1**: $\alpha_i = \alpha_{i(\mathrm{K})}$

$$\text{if} \quad i = h \quad \text{then} \quad S_{G_{Y_j^{(h)}Y_j^{(h)}},i}(\omega) = \left. \frac{\partial G_{Y_j^{(h)}Y_j^{(h)}}(\boldsymbol{\alpha}, \omega)}{\partial \alpha_i} \right|_{\boldsymbol{\alpha}=\mathbf{0}} = 2G^{(0)}_{Y_j^{(h)}Y_j^{(h)}}(\omega) + \mathbf{r}_j^{(h)\mathrm{T}} \mathbf{P}_h(\omega) \mathbf{r}_j^{(h)} \tag{38}$$

$$\text{if} \quad i \neq h \quad \text{then} \quad S_{G_{Y_j^{(h)}Y_j^{(h)}},i}(\omega) = \left. \frac{\partial G_{Y_j^{(h)}Y_j^{(h)}}(\boldsymbol{\alpha}, \omega)}{\partial \alpha_i} \right|_{\boldsymbol{\alpha}=\mathbf{0}} = \mathbf{r}_j^{(h)\mathrm{T}} \mathbf{P}_i(\omega) \mathbf{r}_j^{(h)} \tag{39}$$

where $G^{(0)}_{Y_j^{(h)}Y_j^{(h)}}(\omega)$ is the nominal one-sided *PSD* function of the selected stress process, given by Eq. (25) with $\boldsymbol{\alpha} = \mathbf{0}$. Furthermore, in the previous equations the matrix $\mathbf{P}_i(\omega)$ is defined as

$$\mathbf{P}_i(\omega) = \mathbf{S}_i^*(\omega) \mathbf{G}_{\tilde{\mathbf{X}}_{\mathbf{F}}\tilde{\mathbf{X}}_{\mathbf{F}}}(\omega) \mathbf{H}_0^{\mathrm{T}}(\omega) + \mathbf{H}_0^*(\omega) \mathbf{G}_{\tilde{\mathbf{X}}_{\mathbf{F}}\tilde{\mathbf{X}}_{\mathbf{F}}}(\omega) \mathbf{S}_i^{\mathrm{T}}(\omega) \tag{40}$$

with

$$\mathbf{S}_i(\omega) = \left. \frac{\partial \mathbf{H}(\boldsymbol{\alpha}, \omega)}{\partial \alpha_{(\mathrm{K})i}} \right|_{\boldsymbol{\alpha}=\mathbf{0}} = -(1 + \mathrm{j}c_1\omega) \mathbf{H}_0(\omega)\, \mathbf{K}_i\, \mathbf{H}_0(\omega) \tag{41}$$

where $\mathbf{K}_i$ is given by Eq.(17a) and

$$\mathbf{H}_0(\omega) = \left[ -\omega^2 \mathbf{M} + \mathrm{j}\omega \mathbf{C}_0 + \mathbf{K}_0 \right]^{-1} \tag{42}$$

is the nominal *FRF* matrix.

**Case 2**: $\alpha_i = \alpha_{i(\mathrm{M})}$

$$S_{G_{Y_j^{(h)}Y_j^{(h)},i}}(\omega) = \left. \frac{\partial G_{Y_j^{(h)}Y_j^{(h)}}(\boldsymbol{\alpha}, \omega)}{\partial \alpha_i} \right|_{\boldsymbol{\alpha}=\mathbf{0}} = \mathbf{r}_j^{(h)\mathrm{T}} \mathbf{Q}_i(\omega) \mathbf{r}_j^{(h)} \tag{43}$$

where

$$\mathbf{Q}_i(\omega) = \mathbf{T}_i^*(\omega) \mathbf{G}_{\tilde{\mathbf{X}}_\mathbf{F}\tilde{\mathbf{X}}_\mathbf{F}}(\omega) \mathbf{H}_0^{\mathrm{T}}(\omega) + \mathbf{H}_0^*(\omega) \mathbf{G}_{\tilde{\mathbf{X}}_\mathbf{F}\tilde{\mathbf{X}}_\mathbf{F}}(\omega) \mathbf{T}_i^{\mathrm{T}}(\omega) \tag{44}$$

with

$$\mathbf{T}_i(\omega) = \left. \frac{\partial \mathbf{H}(\boldsymbol{\alpha}, \omega)}{\partial \alpha_{(\mathrm{M})i}} \right|_{\boldsymbol{\alpha}=\mathbf{0}} = -(\mathrm{j}c_0\omega - \omega^2) \mathbf{H}_0(\omega)\, \mathbf{M}_i\, \mathbf{H}_0(\omega) \tag{45}$$

$\mathbf{M}_i$ being defined by Eq. (17b).

Once $S_{G_{Y_j^{(h)}Y_j^{(h)},i}}(\omega)$ is evaluated (Eqs.(38), (39) or (43)), substitution into Eq.(37) yields the $i-\mathrm{th}$ sensitivity of the spectral moments of the interval stress random process $Y_j^{(h)}(\boldsymbol{\alpha}^I, t)$.

The knowledge of the sensitivity $S_{L_{Y_{j,\max}^{(h)}},i}$ defined in Eq.(33) allows us to predict the influence of a small variation of the $i-\mathrm{th}$ uncertain parameter $\alpha_i$ on the *interval reliability function* $L_{Y_{j,\max}^{(h)}}(\boldsymbol{\alpha}^I, b, T)$. Specifically, within a small range around $\boldsymbol{\alpha} = \mathbf{0}$, $L_{Y_{j,\max}^{(h)}}(\boldsymbol{\alpha}^I, b, T)$ is a monotonic increasing or decreasing function of $\alpha_i \in \alpha_i^I = \left[\underline{\alpha}_i, \overline{\alpha}_i\right]$ depending on whether $S_{L_{Y_{j,\max}^{(h)}},i} > 0$ or $S_{L_{Y_{j,\max}^{(h)}},i} < 0$, and its bounds, therefore, correspond to suitable combinations of the endpoints of the uncertain parameter, $\underline{\alpha}_i$ and $\overline{\alpha}_i$. Relying on the monotonic increasing or decreasing behaviour predicted by studying the sign of sensitivities, the combinations of the extreme values of the uncertain parameters which yield accurate estimates of the *LB* and *UB* of the *interval reliability*

*function* $L_{Y_{j,\max}^{(h)}}(\boldsymbol{\alpha}^I, b, T)$, denoted as $\alpha_{Y_{j,\max}^{(h)},i}^{(\mathrm{LB})}$ and $\alpha_{Y_{j,\max}^{(h)},i}^{(\mathrm{UB})}$, $(i=1,2,\ldots,r)$, can be identified as follows:

$$\begin{aligned} &\text{if } S_{L_{Y_{j,\max}^{(h)}},i} > 0, \quad \text{then} \quad \alpha_{Y_{j,\max}^{(h)},i}^{(\mathrm{UB})} = \overline{\alpha}_i, \quad \alpha_{Y_{j,\max}^{(h)},i}^{(\mathrm{LB})} = \underline{\alpha}_i; \\ &\text{if } S_{L_{Y_{j,\max}^{(h)}},i} < 0, \quad \text{then} \quad \alpha_{Y_{j,\max}^{(h)},i}^{(\mathrm{UB})} = \underline{\alpha}_i, \quad \alpha_{Y_{j,\max}^{(h)},i}^{(\mathrm{LB})} = \overline{\alpha}_i. \end{aligned} \tag{46a,b}$$

Such combinations can be collected into the following two vectors:

$$\begin{aligned} \boldsymbol{\alpha}_{Y_{j,\max}^{(h)}}^{(\mathrm{LB})} &= \left[ \alpha_{Y_{j,\max}^{(h)},1}^{(\mathrm{LB})} \quad \alpha_{Y_{j,\max}^{(h)},2}^{(\mathrm{LB})} \quad \ldots \quad \alpha_{Y_{j,\max}^{(h)},r}^{(\mathrm{LB})} \right]^{\mathrm{T}}; \\ \boldsymbol{\alpha}_{Y_{j,\max}^{(h)}}^{(\mathrm{UB})} &= \left[ \alpha_{Y_{j,\max}^{(h)},1}^{(\mathrm{UB})} \quad \alpha_{Y_{j,\max}^{(h)},2}^{(\mathrm{UB})} \quad \ldots \quad \alpha_{Y_{j,\max}^{(h)},r}^{(\mathrm{UB})} \right]^{\mathrm{T}}. \end{aligned} \tag{47a,b}$$

Finally, the *LB* and *UB* of the *interval reliability function* for the interval stress random process $Y_j^{(h)I}(t)$ can be obtained by evaluating Eq.(28) for $\boldsymbol{\alpha} = \boldsymbol{\alpha}_{Y_{j,\max}^{(h)}}^{(\mathrm{LB})}$ and $\boldsymbol{\alpha} = \boldsymbol{\alpha}_{Y_{j,\max}^{(h)}}^{(\mathrm{UB})}$, respectively:

$$\begin{aligned} \underline{L}_{Y_{j,\max}^{(h)}}(b,T) &\approx \exp\left\{ -T\, \nu_{Y_j^{(h)}}^{+}(\boldsymbol{\alpha}_{Y_{j,\max}^{(h)}}^{(\mathrm{LB})}) \exp\left[ -\frac{\left( b - \left| \mu_{Y_j^{(h)}}(\boldsymbol{\alpha}_{Y_{j,\max}^{(h)}}^{(\mathrm{LB})}) \right| \right)^2}{2\lambda_{0,Y_j^{(h)}}(\boldsymbol{\alpha}_{Y_{j,\max}^{(h)}}^{(\mathrm{LB})})} \right] \right\}; \\ \overline{L}_{Y_{j,\max}^{(h)}}(b,T) &\approx \exp\left\{ -T\, \nu_{Y_j^{(h)}}^{+}(\boldsymbol{\alpha}_{Y_{j,\max}^{(h)}}^{(\mathrm{UB})}) \exp\left[ -\frac{\left( b - \left| \mu_{Y_j^{(h)}}(\boldsymbol{\alpha}_{Y_{j,\max}^{(h)}}^{(\mathrm{UB})}) \right| \right)^2}{2\lambda_{0,Y_j^{(h)}}(\boldsymbol{\alpha}_{Y_{j,\max}^{(h)}}^{(\mathrm{UB})})} \right] \right\}. \end{aligned} \tag{48a,b}$$

Summarizing, the sensitivity-based procedure requires only two stochastic analyses of the structure for assigned values of the uncertain parameters given by Eqs (47a,b) in order to evaluate the mean-value and spectral moments of zero- and second-order of the interval stress random process $Y_j^{(h)}(\boldsymbol{\alpha}^I, t)$ entering the definition of the *CDF* (see Eq. (28)).

Equations (48a,b) provide the right bound and left bound of the p-box (see Eq. (27)) which defines the range of the *interval reliability function* resulting from the fluctuations of the uncertain Young's moduli and mass densities within their intervals.

The worst case scenario, which guarantees a conservative design, corresponds to the *LB* of the *interval CDF* (see Eq. (48a)) and the associated *UB* of the *interval failure probability*. The latter can be evaluated substituting Eq.(48a) into Eq. (32b), i.e.:

$$\bar{P}_{f,Y_{j,\max}^{(h)}}(b,T) = 1 - \underline{L}_{Y_{j,\max}^{(h)}}(b,T) = 1 - L_{Y_{j,\max}^{(h)}}(\boldsymbol{\alpha}, b, T)\Big|_{\boldsymbol{\alpha}=\boldsymbol{\alpha}_{Y_{j,\max}^{(h)}}^{(\mathrm{LB})}} \tag{49a,b}$$

The knowledge of the sensitivities of the interval *CDF* of the *extreme value* stress random process $Y_{j,\max}^{(h)}(\boldsymbol{\alpha}^I, T)$ in Eq. (33) can also be exploited to enhance the computational efficiency of the proposed procedure. As known, sensitivity analysis allows identifying the most influential parameters on the response quantity of interest. To this aim, the so-called *function of sensitivity* of the *CDF* $L_{Y_{j,\max}^{(h)}}^{I}(b,T)$ is evaluated:

$$\varphi_{(\mathrm{Q})i,L_{Y_{j,\max}^{(h)}}}(b,T)(\%) = \frac{S_{L_{Y_{j,\max}^{(h)}},i}(b,T)}{L_{Y_{j,\max}^{(h)}}^{(0)}(b,T)}\Delta\alpha_{(\mathrm{Q})i} \times 100, \quad \mathrm{Q=K,\ M} \tag{50}$$

where $S_{L_{Y_{j,\max}^{(h)}},i}(b,T)$ is the $i-$th sensitivity of the *interval CDF* $L_{Y_{j,\max}^{(h)}}(\boldsymbol{\alpha}^I, b, T)$, defined in Eq. (33); $L_{Y_{j,\max}^{(h)}}^{(0)}(b,T)$ is the *CDF* pertaining to the nominal system; $\Delta\alpha_{(\mathrm{Q})i}$ denotes the deviation amplitude of the $i-$th interval parameter $\alpha_i^I = \Delta\alpha_{(\mathrm{Q})i}\hat{e}_i^I$ where the subscript in parenthesis identifies the stiffness (Q=K) and mass parameters (Q=M). The *function of sensitivity* represents a percentage measure of the influence of the generic interval variable $\alpha_i^I$ on the *CDF* of the selected *extreme value* stress process. This implies that the crucial uncertain parameters are those characterized by higher values of the *function of sensitivity*. The least influential parameters can be reasonably assumed deterministic and set equal to their nominal values.

It is worth remarking that, for randomly excited structures, the assumption of monotonic dependency of response statistics on the mass and stiffness parameters is not always satisfied, especially when resonance conditions occur (see e.g. [36],[52]) and large degrees of uncertainty are

considered. In such situations, which are not very common in practical engineering, the accuracy of the proposed approach might worsen since the bounds of the *interval CDF* of the selected response process are attained for intermediate values of the interval parameters. As a preliminary step of the presented procedure, the monotonic behaviour of the response quantity of interest with respect to the $i$-th uncertain parameter $\alpha_i \in \alpha_i^I = [\underline{\alpha}_i, \overline{\alpha}_i]$ should be checked by verifying that the sign of the sensitivity to $\alpha_i$ remains unchanged over the pertinent interval (see e.g., [57]).

## 4. BOUNDS OF THE INTERVAL FRACTILES

For structures with uncertain-but-bounded parameters, the so-called *fractile* of order *p*, i.e. the response level which has a specified probability, *p*, of not being exceeded during the observation time $[0,T]$, has an interval nature as well [46], [50].

The *LB* and *UB* of the *interval fractile* of order *p*, $Z^I_{Y^{(h)}_{j,\max}}(p,T) \equiv Z_{Y^{(h)}_{j,\max}}(\boldsymbol{\alpha}^I, p, T)$, of the interval stress random process $Y_j^{(h)}(\boldsymbol{\alpha}^I, t)$ can be computed by solving the following nonlinear equations [46],[50]:

$$p = \overline{L}_{Y^{(h)}_{j,\max}}\left(\underline{Z}_{Y^{(h)}_{j,\max}}(p,T), T\right); \quad p = \underline{L}_{Y^{(h)}_{j,\max}}\left(\overline{Z}_{Y^{(h)}_{j,\max}}(p,T), T\right) \tag{51a,b}$$

where $\overline{L}_{Y^{(h)}_{j,\max}}$ and $\underline{L}_{Y^{(h)}_{j,\max}}$ are the *UB* and *LB* of the interval *CDF* (see Eqs. (48a,b)).

Alternatively, the *interval fractile* of order *p* can be defined by interval extension of the approximate analytical expression holding under the Poisson assumption of independent up-crossings [58], i.e.:

$$Z^I_{Y^{(h)}_{j,\max}}(p,T) \equiv Z_{Y^{(h)}_{j,\max}}(\boldsymbol{\alpha}^I, p, T) = \psi_{Y_j^{(h)}}(p,T;\boldsymbol{\alpha}^I)\sqrt{\lambda_{0,Y_j^{(h)}}(\boldsymbol{\alpha}^I)} + \left|\mu_{Y_j^{(h)}}(\boldsymbol{\alpha}^I)\right| \tag{52}$$

where

$$\psi^{I}_{Y_j^{(h)}}(p,T) \equiv \psi_{Y_j^{(h)}}(p,T;\boldsymbol{\alpha}^I) = \sqrt{2\ln\left(\nu^{+}_{Y_j^{(h)}}(\boldsymbol{\alpha}^I)T\right)} - \frac{\ln[-\ln(p)]}{\sqrt{2\ln\left(\nu^{+}_{Y_j^{(h)}}(\boldsymbol{\alpha}^I)T\right)}}. \tag{53}$$

Notice that Eq. (52) involves only the mean-value and spectral moments of zero- and second-order of the interval stress random process $Y_j^{(h)}(\boldsymbol{\alpha}^I,t)$.

The sensitivity-based procedure outlined above for the *interval reliability function* is herein applied to evaluate the *LB* and *UB* of the *interval fractile* of order *p* defined by Eq. (52).

By applying the chain rule of differentiation, the following expression of the $i-$th sensitivity of the *interval fractile* of order *p* is obtained [50]:

$$\begin{aligned} S_{Z_{Y_{j,\max}^{(h)}},i} = \left.\frac{\partial Z_{Y_{j,\max}^{(h)}}(\boldsymbol{\alpha},p,T)}{\partial\alpha_i}\right|_{\boldsymbol{\alpha}=\mathbf{0}} &= \frac{1}{2\sqrt{\lambda^{(0)}_{0,Y_j^{(h)}}}\sqrt{2\ln(\nu^{+(0)}_{Y_j^{(h)}}T)}} \\ &\times\left\{2\ln(\nu^{+(0)}_{Y_j^{(h)}}T) - 1 - \ln[-\ln(p)]\left[1+\frac{1}{2\ln(\nu^{+(0)}_{Y_j^{(h)}}T)}\right]\right\} S_{\lambda_{0,Y_j^{(h)}},i} \\ &+ \frac{\sqrt{\lambda^{(0)}_{0,Y_j^{(h)}}}}{2\lambda^{(0)}_{2,Y_j^{(h)}}\sqrt{2\ln(\nu^{+(0)}_{Y_j^{(h)}}T)}}\left[1+\frac{\ln[-\ln(p)]}{2\ln(\nu^{+(0)}_{Y_j^{(h)}}T)}\right] S_{\lambda_{2,Y_j^{(h)}},i} + \frac{\left|\mu^{(0)}_{Y_j^{(h)}}\right|}{\mu^{(0)}_{Y_j^{(h)}}} S_{\mu_{Y_j^{(h)}},i} \end{aligned} \tag{54}$$

where $S_{\mu_{Y_j^{(h)}},i}$ and $S_{\lambda_{\ell,Y_j^{(h)}},i}$ $(\ell=0,2)$ are the $i-$th sensitivities of the interval mean-value and spectral moments of $Y_j^{(h)I}(t)$ defined in the previous section; $\mu^{(0)}_{Y_j^{(h)}}$ and $\lambda^{(0)}_{\ell,Y_j^{(h)}}$ $(\ell=0,2)$ denote the nominal mean-value and spectral moments of the selected stress process; and $\nu^{+(0)}_{Y_j^{(h)}}$ is defined by Eq.(29) for $\boldsymbol{\alpha}=\mathbf{0}$.

The combinations of the extreme values of the uncertain parameters which provide accurate estimates of the bounds of the *interval fractile* of order *p* of the interval stress random process $Y_j^{(h)I}(t)$, herein denoted by $\alpha^{(\mathrm{LB})}_{Z_{Y_j^{(h)},\max},i}$ and $\alpha^{(\mathrm{UB})}_{Z_{Y_j^{(h)},\max},i}$, $(i=1,2,\ldots,r)$, can be evaluated by examining the sign of the pertinent sensitivities $S_{Z_{Y_{j,\max}^{(h)}},i}$ (Eq.(54)), as follows:

$$\text{if } S_{Z_{Y_{j,\max}^{(h)},i}} > 0, \quad \text{then} \quad \alpha^{(\mathrm{UB})}_{Z_{Y_j^{(h)},\max},i} = \overline{\alpha}_i, \ \alpha^{(\mathrm{LB})}_{Z_{Y_j^{(h)},\max},i} = \underline{\alpha}_i;$$
$$\text{if } S_{Z_{Y_{j,\max}^{(h)},i}} < 0, \quad \text{then} \quad \alpha^{(\mathrm{UB})}_{Z_{Y_j^{(h)},\max},i} = \underline{\alpha}_i, \ \alpha^{(\mathrm{LB})}_{Z_{Y_j^{(h)},\max},i} = \overline{\alpha}_i. \tag{55a,b}$$

Such combinations can be gathered into the following two vectors:

$$\boldsymbol{\alpha}^{(\mathrm{LB})}_{Z_{Y_j^{(h)},\max}} = \left[ \alpha^{(\mathrm{LB})}_{Z_{Y_j^{(h)},\max},1} \quad \alpha^{(\mathrm{LB})}_{Z_{Y_j^{(h)},\max},2} \quad \dots \quad \alpha^{(\mathrm{LB})}_{Z_{Y_j^{(h)},\max},r} \right]^{\mathrm{T}};$$
$$\boldsymbol{\alpha}^{(\mathrm{UB})}_{Z_{Y_j^{(h)},\max}} = \left[ \alpha^{(\mathrm{UB})}_{Z_{Y_j^{(h)},\max},1} \quad \alpha^{(\mathrm{UB})}_{Z_{Y_j^{(h)},\max},2} \quad \dots \quad \alpha^{(\mathrm{UB})}_{Z_{Y_j^{(h)},\max},r} \right]^{\mathrm{T}}. \tag{56a,b}$$

The *LB* and *UB* of the *interval fractile* of order *p* of the interval stress random process $Y_h^I(t)$ can be estimated by evaluating Eq. (52) for $\boldsymbol{\alpha} = \boldsymbol{\alpha}^{(\mathrm{LB})}_{Z_{Y_j^{(h)},\max}}$ and $\boldsymbol{\alpha} = \boldsymbol{\alpha}^{(\mathrm{UB})}_{Z_{Y_j^{(h)},\max}}$, respectively:

$$\underline{Z}_{Y_{j,\max}^{(h)}}(p,T) = \psi_{Y_j^{(h)}}\left(p,T;\boldsymbol{\alpha}^{(\mathrm{LB})}_{Z_{Y_j^{(h)},\max}}\right)\sqrt{\lambda_{0,Y_j^{(h)}}(\boldsymbol{\alpha}^{(\mathrm{LB})}_{Z_{Y_j^{(h)},\max}})} + \left|\mu_{Y_j^{(h)}}\left(\boldsymbol{\alpha}^{(\mathrm{LB})}_{Z_{Y_j^{(h)},\max}}\right)\right|;$$
$$\overline{Z}_{Y_{j,\max}^{(h)}}(p,T) = \psi_{Y_j^{(h)}}\left(p,T;\boldsymbol{\alpha}^{(\mathrm{UB})}_{Z_{Y_j^{(h)},\max}}\right)\sqrt{\lambda_{0,Y_j^{(h)}}(\boldsymbol{\alpha}^{(\mathrm{UB})}_{Z_{Y_j^{(h)},\max}})} + \left|\mu_{Y_j^{(h)}}(\boldsymbol{\alpha}^{(\mathrm{UB})}_{Z_{Y_j^{(h)},\max}})\right|. \tag{57a,b}$$

These bounds enclose the values of the interval stress random process $Y_j^{(h)I}(t)$ having probability *p* of not being exceeded during the observation time $[0,T]$. In order to ensure a conservative design, the worst case scenario, corresponding to the *UB* of the selected *fractile* of order *p*, should be considered.

The flowchart in Fig. 1 summarizes the proposed sensitivity-based procedure for evaluating the bounds of the *interval reliability function* and of the *interval fractile* of order *p* of the selected response process.

## 5. NUMERICAL APPLICATIONS

The effectiveness of the proposed procedure is assessed by performing *first-passage* reliability analysis of two structures with interval uncertainties subjected to wind excitation modelled as a

stationary Gaussian multi-correlated random process: a steel telecommunication antenna mast and a ten-story shear-type frame.

The model of wind loads assumed for both the selected case-studies is briefly summarized in the following. The along wind force ($x$-direction) exerted on the $i$-th node at height $z_i$ of the discretized structure is defined by the well-known formula [59]:

$$F_{x,i}(z_i,t) = \frac{1}{2}\rho C_D A_i w_s^2(z_i) + \rho C_D A_i \tilde{W}(z_i,t) w_s(z_i) \tag{58}$$

where the contribution of the nodal velocities of the structure and the square of the fluctuating component of wind speed have been neglected. In Eq. (58), $\rho = 1.25$ kg/m$^3$ is the air density; $C_D$ is the drag coefficient; $A_i$ is the tributary area of the $i$-th node; $w_s$ is the mean wind velocity which is assumed to vary with the elevation $z$ following a power law, i.e.:

$$w_s(z) = w_{s,10}\left(\frac{z}{10}\right)^{\gamma} \tag{59}$$

where $w_{s,10}$ is the mean wind speed measured at height $z = 10\,\text{m}$ above ground and $\gamma$ is a coefficient depending on surface roughness, herein taken equal to $w_{s,10} = 25$ m/s and $\gamma = 0.3$, respectively. Furthermore, $\tilde{W}(z,t)$ denotes the fluctuating component of wind velocity field, which is modelled as a zero-mean stationary Gaussian random field, fully described from a probabilistic point of view by the one-sided *PSD* function [60]:

$$G_{\tilde{W}\tilde{W}}(\omega) = 4K_0 w_{s,10}^2 \frac{\chi^2}{\omega\left(1+\chi^2\right)^{4/3}} \tag{60}$$

where $K_0$ is the non-dimensional roughness coefficient, herein set equal to $K_0 = 0.03$, and $\chi = b_1\omega/(\pi w_{s,10})$ with $b_1 = 600$ m. The vector $\tilde{\mathbf{W}}(t)$ collecting wind velocity fluctuations at the wind-exposed nodes located at different heights $z_i$ is characterized from a probabilistic point of

view by the one-sided *PSD* function matrix $\mathbf{G}_{\tilde{\mathbf{W}}\tilde{\mathbf{W}}}(\omega)$. If the imaginary part (*q*-spectrum) [59] is neglected, the cross-*PSD* components of $\mathbf{G}_{\tilde{\mathbf{W}}\tilde{\mathbf{W}}}(\omega)$ can be expressed as follows:

$$G_{\tilde{W}_i\tilde{W}_j}(z_i, z_j; \omega) = G_{\tilde{W}\tilde{W}}(\omega)\, f_{ij}(\omega) \tag{61}$$

where $f_{ij}(\omega)$ is the so-called *coherence function*, defined as

$$f_{ij}(\omega) = \mathrm{Exp}\left\{ -\frac{|\omega|\sqrt{C_z^2 (z_i - z_j)^2}}{\pi\left[ w_s(z_i) + w_s(z_j) \right]} \right\} \tag{62}$$

with $C_z$ denoting an appropriate decay coefficient to be determined experimentally, herein set equal to $C_z = 10$.

Preliminary numerical investigations, omitted for conciseness, have shown that, for the selected case studies, the spectral moments of the response quantity of interest are monotonic functions of each uncertain mass and stiffness parameter. Thus, the presented sensitivity-based procedure is expected to provide very accurate results. For validation purposes, the proposed bounds of the *interval reliability function* and of the *interval fractiles* of order *p* of the selected stress process are compared with those provided by the *vertex method* [61]. The latter is a computationally intensive combinatorial procedure which provides the exact bounds of the solution when the latter is a monotonic function of the uncertain parameters. In the context of *first-passage* reliability analysis, the *vertex method* requires to evaluate the *reliability function* for all the $2^r$ possible combinations of the endpoints of the $r$ uncertain parameters. Then, for each barrier level $b$, the *LB* and *UB* of the *interval reliability function* are obtained as the minimum and maximum among the $2^r$ values pertaining to the *vertex* analysis.

### 5.1 Steel telecommunication antenna mast under wind excitation

The first case study is represented by the 28.50 m high steel communication antenna mast subjected to wind excitation shown in Fig.2a. The antenna is discretized into $N^{(e)}=19$ two-node Euler-Bernoulli beam FEs resulting in a $n=38$ DOFs system (Fig. 2b). A lumped mass model is assumed. The properties of the FE model of the antenna are listed in Table 1, where the masses lumped at nodes and the tributary areas $A_i$ entering the definition of wind loads $F_{x,i}(z_i,t)$ (see Eq. (58)) are also reported. The nominal Young's modulus is set equal to $E_0$=210 GPa for the whole structure. The values $c_0=0.149575\,\mathrm{s}^{-1}$ and $c_1=0.00316358\,\mathrm{s}$ are assumed for the Rayleigh damping constants in Eq. (18) in such a way that the modal damping ratio of the first and third modes of the nominal structure is $\zeta_0=0.01$. The fundamental period of the nominal structure is $T_0=0.723\,\mathrm{s}$.

It is assumed that Young's modulus of the material is affected by uncertainty. In a first stage, in order to make comparisons with the *vertex method* computationally feasible, only the first $r_{\mathrm{K}}=12$ FEs (see Fig. 2b) are assumed to be characterized by interval Young's moduli i.e. $E^{(i)I}=E_0\left(1+\Delta\alpha\hat{e}^I_{(\mathrm{K})i}\right)$, $(i=1,2,\ldots,r_{\mathrm{K}}=12)$, where the same deviation amplitude is considered. Under this assumption, the application of the *vertex method* involves $2^{r_{\mathrm{K}}}=2^{12}$ stochastic analyses of the structure while the proposed method requires to evaluate the *reliability function* only twice, regardless of the number of uncertain parameters. The maximum interval axial stress, $Y_1^{(1)I}(t)$, at the antenna base section, i.e. at node 1 of FE 1, is assumed as the response quantity responsible of structural failure. To predict the range of structural performance, the bounds of the *interval reliability function*, $L^I_{Y^{(1)}_{1,\max}}(b,T)$, (see Eq. (28)) and of the *interval failure probability* $P^I_{f,Y^{(1)}_{1,\max}}(b,T)$ (see Eq. (31)) are evaluated. The observation time is assumed equal to $T=1000T_0$, $T_0$ being the fundamental period of the structure with nominal Young's moduli.

In Figs. 3 and 4, the proposed *LB* and *UB* of $L^I_{Y^{(1)}_{1,\max}}(b,T)$ and $P^I_{f,Y^{(1)}_{1,\max}}(b,T)$ (the latter in semi-logarithmic scale) are compared with those provided by the *vertex method*. Two different deviation amplitudes of the uncertain parameters, $\Delta\alpha = 0.10$ and $\Delta\alpha = 0.20$, are considered. The nominal *CDF*, $L^{(0)}_{Y^{(1)}_{1,\max}}(b,T)$, and *failure probability*, $P^{(0)}_{f,Y^{(1)}_{1,\max}}(b,T)$, are also reported. An excellent agreement between the proposed sensitivity-based procedure and the *vertex method* can be observed. As expected, the region describing structural performance becomes wider as the degree of uncertainty increases. The deviation of the *LB* and *UB* of both the *CDF* and *failure probability* from the nominal solution proves that assuming the nominal value of Young's moduli may lead to misleading predictions of structural safety level.

In order to provide a measure of the dispersion of structural performance around the midpoint value, the so-called *coefficient of interval uncertainty* of the interval *CDF* $L^I_{Y^{(1)}_{1,\max}}(b,T)$ can be estimated, i.e.:

$$c.i.u.[L^I_{Y^{(1)}_{1,\max}}(b,T)] = \frac{\overline{L}_{Y^{(1)}_{1,\max}}(b,T) - \underline{L}_{Y^{(1)}_{1,\max}}(b,T)}{\overline{L}_{Y^{(1)}_{1,\max}}(b,T) + \underline{L}_{Y^{(1)}_{1,\max}}(b,T)}. \tag{63}$$

For instance, assuming a barrier level $b = 90.00$ MPa, based on the proposed bounds of the interval *CDF* $L^I_{Y^{(1)}_{1,\max}}(b,T)$, shown in Figs. 3 and 4, the $c.i.u.[L^I_{Y^{(1)}_{1,\max}}(b,T)]$ takes the values $0.05$ and $0.11$ for $\Delta\alpha = 0.10$ and $\Delta\alpha = 0.20$, respectively.

In order to predict the influence of a small change of Young's moduli on the performance of the telecommunication antenna mast, the *function of sensitivity* of the *CDF* $L^I_{Y^{(1)}_{1,\max}}(b,T)$ is evaluated (see Eq. (50)) under the assumption that all Young's moduli are described by intervals. In Fig. 5, the *functions of sensitivity* $\varphi_{(\mathrm{K})i,L_{Y^{(1)}_{1,\max}}}(b,T)$ of $L^I_{Y^{(1)}_{1,\max}}(b,T)$ with respect to the fluctuations $\alpha^I_{(\mathrm{K})i} = \Delta\alpha\hat{e}^I_{(\mathrm{K})i}$ of a selected number of interval Young's moduli

$E_i^I = E_0(1+\alpha_{(\mathrm{K})i}^I) = E_0(1+\Delta\alpha\hat{e}_{(\mathrm{K})i}^I)$, $(i=1,2,\ldots,8,12,13,14,16,17)$ versus the deterministic barrier level $b$ are plotted ($\Delta\alpha = 0.10$). For the sake of clarity, the *functions of sensitivity* with respect to the fluctuations of the remaining Young's moduli are omitted. It is observed that the most influential Young's moduli are those of FEs 1 and 16 for any value of the barrier level. A close inspection of Fig. 5 also shows that a small increase of Young's moduli of the first eight FEs would produce an increment of structural reliability since the pertinent *functions of sensitivity* are positive. Conversely, a small increase of Young's moduli of FEs $12,13,14,16,17$ would lead to a lower safety level.

Figure 6 shows the values of the *function of sensitivity* $\varphi_{(\mathrm{K})i,L_{Y_{1,\max}^{(1)}}}(b,T)$ of the *CDF* $L_{Y_{1,\max}^{(1)}}^I(b,T)$ with respect to the fluctuations $\alpha_{(\mathrm{K})i}^I = \Delta\alpha\hat{e}_{(\mathrm{K})i}^I$ $(i=1,2,\ldots,19)$ of Young's moduli of all the FEs for a given barrier level $b = 89.44$ MPa, selected as the one having a probability $p = 0.50$ of not being exceeded during the observation time $T = 1000T_0$ when all the uncertain parameters are set equal to the nominal value. The results reported in Fig. 6 allow ranking the uncertain parameters from the most to the least influential ones based on the corresponding absolute value of the *function of sensitivity*. It can be readily inferred that the least influential parameters are Young's moduli of FEs 11,9,15,18,10,19, listed in decreasing order of importance. Thus, in order to enhance the computational efficiency of the proposed method, such parameters can be reasonably set equal to their nominal values and only $r_K = 13$ uncertain parameters, $E^{(i)I} = E_0\left(1+\Delta\alpha\hat{e}_{(\mathrm{K})i}^I\right)$, $(i=1,2,\ldots,8,12,13,14,16,17)$ (see Fig. 6), out of $r_K = N^{(e)} = 19$ might be retained in reliability analysis.

In Fig. 7, the bounds of the *interval reliability function* $L_{Y_{1,\max}^{(1)}}^I(b,T)$ evaluated by applying the proposed sensitivity-based approach considering Young's moduli of all the $r_{\mathrm{K}} = N^{(e)} = 19$ FEs as uncertain (full) are contrasted with the ones computed retaining only the $r_K = 13$ most influential

uncertain parameters (reduced) identified by sensitivity analysis (see Fig. 6). For comparison purpose, the bounds pertaining to the structure with the first $r_K = 6$ most influential uncertain Young's moduli $E^{(i)I} = E_0\left(1+\Delta\alpha\hat{e}^I_{(\mathrm{K})i}\right)$, $(i = 1,2,3,4,5,16)$, are also plotted. Also in this case, two different deviation amplitudes of the uncertain parameters, $\Delta\alpha = 0.10$ and $\Delta\alpha = 0.20$, are considered. It can be observed that the left and right bounds of the p-box describing structural performance obtained considering only the first $r_K = 6$ uncertain parameters are enclosed by the bounds pertaining to full uncertainty. This entails that some of the neglected parameters play a crucial role in the prediction of the safety level. Conversely, the region of the *interval CDF* predicted retaining $r_K = 13$ uncertain Young's moduli is almost coincident with the one obtained performing full uncertainty analysis. This implies that the dimension of the uncertainty input space can be reduced to $r_K = 13$ without significantly affecting the accuracy of the results.

In Fig. 8, the bounds of the *interval fractiles* of order $p = 0.50$ and $p = 0.95$ of the *extreme value* stress process $Y^{(1)I}_{1,\max}(T)$ versus the deviation amplitude of the interval Young's moduli $E^{(i)I} = E_0\left(1+\Delta\alpha\hat{e}^I_{(\mathrm{K})i}\right)$, $(i = 1,2,\ldots,r_{\mathrm{K}} = 12)$, of the first $r_{\mathrm{K}} = 12$ FEs (see Fig. 2) are plotted. As expected, the proposed estimates of the *LB* and *UB* are in excellent agreement with the ones provided by the *vertex method*. Furthermore, the region of the *interval fractiles* broadens as the degree of uncertainty of Young's moduli increases.

### 5.2 Ten-story shear-type frame under wind excitation

As second case-study, the ten-story shear-type frame under wind excitation depicted in Fig. 9 is considered. The geometrical properties of the frame are reported in Fig. 9 and Table 2. The mass of the structure is assumed uniformly distributed on each floor with nominal value $m_{0i} = m_0 = 60$ t ( $i = 1,2,\ldots,10$). The structure is made of concrete with nominal Young's modulus $E_0$=25 GPa. Wind loads $F_{x,i}(z_i,t)$ exerted at each floor located at height $z_i$ are defined by Eq. (58) with

tributary areas $A_i = 12.00\ \mathrm{m}^2$, $(i = 1,2,\ldots,9)$, and $A_{10} = 6.00\ \mathrm{m}^2$. The values $c_0 = 0.483378\ \mathrm{s}^{-1}$ and $c_1 = 0.00315051\mathrm{s}$ are assumed for the Rayleigh damping constants in Eq. (18) in such a way that the modal damping ratio of the first and third modes of the nominal structure is $\zeta_0 = 0.05$. The fundamental period of the nominal structure is $T_0 = 1.055\ \mathrm{s}$.

Young's modulus of the material of two columns at the same floor is assumed to be described by the same interval variable $E^{(i)I} = E_0\left(1 + \Delta\alpha\hat{e}^I_{(\mathrm{K})i}\right)$, $(i = 1,2,\ldots,r_{\mathrm{K}} = 10)$, as a result of the actual concrete casting. Floor masses are also described as interval variables $m^{(i)I} = m_0\left(1 + \Delta\alpha\hat{e}^I_{(\mathrm{M})i}\right)$, $(i = 1,2,\ldots,r_{\mathrm{M}} = 10)$. For the sake of simplicity, the same deviation amplitude is assumed for all the uncertain parameters.

The shear stress at the base of column 2, $Y_2^{(2)I}(t)$, is assumed as critical response quantity. The aim of the analysis is the evaluation of the range of the *interval reliability function*, $L^I_{Y^{(2)}_{2,\max}}(b,T)$, and of the *interval fractiles* of order $p = 0.50, 0.95$, $Z^I_{Y^{(2)}_{2,\max}}(p,T)$, of the *extreme value* process $Y^{(2)I}_{2,\max}(T)$, where the observation time is assumed equal to $T = 1000T_0$, $T_0$ being the fundamental period of the nominal structure.

First, the relative importance of the uncertain mass and stiffness parameters on structural performance is investigated by performing sensitivity analysis. Figures 10a and 10b display the *functions of sensitivity* of the *interval reliability function* $L^I_{Y^{(2)}_{2,\max}}(b,T)$ (see Eq. (50)) with respect to the fluctuations of Young's moduli and floor masses, respectively. As expected, the various structural parameters have a different impact on the *CDF*. In particular, it is observed that Young's modulus of the columns of the third floor and the mass of the tenth floor are the most influential ones on the *CDF* $L^I_{Y^{(2)}_{2,\max}}(b,T)$. Also in this case, it is worth remarking that positive values of the *functions of sensitivity* entail that a small increase of the pertinent parameters would produce an increment of structural reliability.

Figures 11a and 11b show the values of the *functions of sensitivity* $\varphi_{(\mathrm{K})i,L_{Y_{2,\max}^{(2)}}}(b,T)$ and $\varphi_{(\mathrm{M})i,L_{Y_{2,\max}^{(2)}}}(b,T)$ of the *CDF* $L^I_{Y_{2,\max}^{(2)}}(b,T)$ with respect to the fluctuations $\alpha^I_{(\mathrm{K})i}=\Delta\alpha\hat{e}^I_{(\mathrm{K})i}$ and $\alpha^I_{(\mathrm{M})i}=\Delta\alpha\hat{e}^I_{(\mathrm{M})i}$, $(i=1,2,\ldots,10)$, of Young's moduli and floor masses for a given barrier level $b=211.92$ MPa which has a probability $p=0.50$ of not being exceeded during the observation time $T=1000T_0$ when all the uncertain parameters are assumed equal to their nominal values. Based on the results reported in Fig. 11a, the uncertain Young's moduli can be ranked from the most to the least influential ones as follows: $E^{(i)I}$, $i=3,4,1,5,2,10,6,9,7,8$. Similarly, by inspection of Fig. 11b, the uncertain floor masses may be listed in decreasing order of influence as follows: $m^{(i)I}$, $i=10,1,9,2,3,4,5,6,8,7$.

A close inspection of Figs. 11a and 11b shows that the *functions of sensitivity* of $L^I_{Y_{2,\max}^{(2)}}(b,T)$ with respect to fluctuations of Young's moduli and masses of the same floor have opposite sign which implies contrasting effects on the reliability of the frame structure. In particular, up to the seventh floor, a small increase of Young's moduli would produce an increment of structural reliability; conversely a small increase of floor masses would lead to a lower safety level. The opposite holds for the parameters associated with the remaining floors. This behaviour is consistent with the impact of a small variation of each uncertain Young's modulus and mass floor on the zero-order spectral moment of the shear stress random process $Y_2^{(2)}(t)$, as can be inferred from Figs. 12 and 13. Indeed, these figures highlight that small increments of the *i*-th Young's modulus and of the *i*-th mass floor around the nominal value, while all the remaining parameters are kept fixed to the nominal value, have an opposite impact on the zero-order spectral moment of the shear stress random process $Y_2^{(2)}(t)$, except for the parameters associated with the eighth floor which actually have a negligible influence.

Relying on the information provided by sensitivity analysis, in order to validate the proposed

approach by comparison with the *vertex method*, the first $r_K = 6$ Young's moduli $E^{(i)I}$, $(i = 1,2,3,4,5,10)$, and $r_M = 6$ masses $m^{(i)I}$, $(i = 1,2,3,4,9,10)$, having the highest influence on the interval *CDF* $L^I_{Y^{(2)}_{2,\max}}(b,T)$ are modelled as interval variables while the remaining parameters are set equal to their nominal values.

Figures 14 and 15 display the comparison between the proposed *LB* and *UB* of the *interval CDF* $L^I_{Y^{(2)}_{2,\max}}(b,T)$ and *failure probability* $P^I_{f,Y^{(2)}_{2,\max}}(b,T)$ (the latter in semi-logarithmic scale) with those provided by the *vertex method*, for two different deviation amplitudes of the uncertain parameters, $\Delta\alpha = 0.10$ and $\Delta\alpha = 0.20$. Also in this case, an excellent matching between the proposed sensitivity-based procedure and the *vertex method* is observed. The width of the region enclosed by the bounds of the *interval CDF* and *failure probability* consistently increases as a higher degree of uncertainty is considered.

Figure 16 shows the bounds of the *interval fractiles* of order $p = 0.50$ and $p = 0.95$ of the *extreme value* stress process $Y^{(2)I}_{2,\max}(T)$ versus the deviation amplitude of the interval Young's moduli and floor masses. The comparison with the bounds obtained by applying the *vertex method* proves the accuracy of the proposed sensitivity-based approach.

The outcomes of sensitivity analysis are also exploited to enhance the computational efficiency of the proposed approach by reducing the dimension of uncertainty. In Fig. 17, the bounds of the *interval reliability function* $L^I_{Y^{(2)}_{2,\max}}(b,T)$ evaluated assuming all Young's moduli and floor masses ($r_K = r_M = 10$) as uncertain (full) are contrasted with the ones computed retaining only the first $r_K = r_M = 6$ and $r_K = r_M = 7$ most influential uncertain Young's moduli and floor masses (reduced) based on the ranking established by sensitivity analysis. In all cases, the bounds are estimated using the proposed sensitivity-based procedure, for two different deviation amplitudes of the uncertain parameters, $\Delta\alpha = 0.10$ and $\Delta\alpha = 0.20$. The bounds of the p-box predicted retaining $r_K = 7$

uncertain Young's moduli and $r_M = 7$ uncertain masses are in excellent agreement with those provided by full uncertainty analysis. It can be observed that the region of structural performance pertaining to the frame structure with $r_K = 6$ uncertain Young's moduli and $r_M = 6$ uncertain masses is slightly less accurate.

## 6. CONCLUSIONS

A sensitivity-based procedure for reliability analysis of finite element modeled structures with interval mass and stiffness subjected to stationary Gaussian multi-correlated random excitation is presented. The formulation is developed in the context of the *first-passage* theory under the Poisson assumption of independent up-crossings of a prescribed threshold. The presented procedure basically consists in identifying suitable combinations of the endpoints of the uncertain structural parameters which yield accurate estimates of the bounds of the *interval reliability function* or *cumulative distribution function* (*CDF*), and of the *interval failure probability* for the selected stress process, as long as monotonic problems are dealt with. This task is achieved by performing a preliminary sensitivity analysis of the *reliability function*. The same approach can be pursued to evaluate the bounds of the *interval fractile* of order *p* of the critical stress process.

The main features of the proposed sensitivity-based procedure may be summarized as follows: *i*) the bounds of the *interval CDF* of the selected stress process are obtained by performing only two stochastic analyses of the structure wherein the uncertain parameters are set equal to the combinations identified by sensitivity analysis; *ii*) for monotonic problems, the presented procedure yields results in excellent agreement with the ones provided by the *vertex method* in spite of the much higher computational efficiency; *iii*) reliability analysis of arbitrary finite element modeled structures involving both mass and stiffness uncertainties can be performed; *iv*) sensitivity analysis provides a deep insight into the impact of mass and stiffness fluctuations on structural performance allowing the identification of the least influential parameters which may be set equal to the nominal

values to enhance the computational efficiency.

Overall the present study provides an efficient tool to define the range of the *interval reliability function* and *interval failure probability* of structures subjected to stationary Gaussian multi-correlated random excitation when only the possible ranges of variability of the uncertain mass and stiffness properties are known with sufficient confidence. The non-intrusive nature of the sensitivity-based procedure allows its efficient implementation with the aid of commercial finite element software.

Ongoing research is aimed at gaining a deeper insight into the *interval first-passage* problem for situations entailing a non-monotonic dependence of the response on the uncertain parameters e.g., resonance conditions or imprecise random loadings (see e.g., [51],[52]).

**Acknowledgments**: The authors are grateful to the two anonymous reviewers for their valuable suggestions on an earlier version of this paper.

The authors gratefully acknowledge financial support from the Italian Ministry of Education, University and Research (MIUR) under the P.R.I.N. 2017 National Grant ‘‘Multiscale Innovative Materials and Structures’’ (Project Code 2017J4EAYB; University of Reggio Calabria Research Unit).

## REFERENCES

[1] B.M. Ayyub, G.J. Klir, Uncertainty modeling and analysis in engineering and the sciences, Chapman & Hall/CRC, Taylor & Francis Group, Boca Raton, 2006.

[2] A. Der Kiureghian, Analysis of structural reliability under parameter uncertainties, Probab. Eng. Mech. 23 (2008), 351–358.

[3] R.B. Corotis, An overview of uncertainty concepts related to mechanical and civil engineering, ASCE-ASME J. Risk Uncertainty Eng. Syst. Part B: Mech. Eng. 1(4) (2015) 040801 (12 pages).

[4] Y. Ben-Haim, A non-probabilistic concept of reliability, Struct. Saf. 14(4), (1994), 227-245.

[5] I. Elishakoff, Essay on uncertainties in elastic and viscoelastic structures: From A. M. Freudenthal's criticisms to modern convex modeling, Comput. Struct. 56(6) (1995) 871–895.

[6] D. Moens, D. Vandepitte, A survey of non-probabilistic uncertainty treatment in finite element analysis, Comput. Methods Appl. Mech. Eng. 194 (2005) 1527-1555.

[7] I. Elishakoff and M. Ohsaki, Optimization and Anti-Optimization of Structures under Uncertainty, Imperial College Press, London, 2010.

[8] I. Elishakoff, Possible limitations of probabilistic methods in engineering, Applied Mechanics Review, 53(2), (2000) 19–36.

[9] R.E. Moore, Interval Analysis, Prentice-Hall, Englewood Cliffs, 1966.

[10] R.E. Moore, R.B. Kearfott and M.J. Cloud, Introduction to Interval Analysis, SIAM, Philadelphia, 2009.

[11] Y. Ben-Haim, I. Elishakoff, Convex Models of Uncertainty in Applied Mechanics, Elsevier, Amsterdam, 1990.

[12] L. Zadeh, Fuzzy sets, Inform Contr. 8 (1965) 338–353.

[13] R.C. Penmetsa and R.V.Grandhi, Efficient estimation of structural reliability for problems with uncertain intervals, Comput. Struct. 80 (2002) 1103–1112.

[14] Z. Qiu, D.Yang and I. Elishakoff, Probabilistic interval reliability of structural systems, Int. J. Solids Struct. 45 (2008) 2850–2860.

[15] H. Zhang, R.L. Mullen and R.L. Muhanna, Interval Monte Carlo methods for structural reliability, Struct. Saf. 32 (2010) 183-190.

[16] J.E. Hurtado and D.A. Alvarez, The encounter of interval and probabilistic approaches to structural reliability at the design point, Comput. Methods Appl. Mech. Eng. 225–228 (2012) 74–94.

[17] H. Zhang, Interval importance sampling method for finite element-based structural reliability assessment under parameter uncertainties, Struct. Saf. 38 (2012) 1–10.

[18] M. Beer, Y. Zhang, S.T. Quek and K.K. Phoon, Reliability analysis with scarce information: comparing alternative approaches in a geotechnical engineering context, Struct. Saf. 41 (2013) 1–10.

[19] J.E. Hurtado, Assessment of reliability intervals under input distributions with uncertain parameters, Probab. Eng. Mech. 32 (2013) 80–92.

[20] C. Jiang, R.G. Bi, G.Y. Lu and X. Han, Structural reliability analysis using non-probabilistic convex model, Comput. Methods Appl. Mech. Eng. 254 (2013) 83–98.

[21] H. Zhang, H. Dai, M. Beer and W. Wang, Structural reliability analysis on the basis of small samples: An interval quasi-Monte Carlo method, Mech. Syst. Signal Process. 37 (2013) 137–151.

[22] D.A. Alvarez and J. E. Hurtado, An efficient method for the estimation of structural reliability intervals with random sets, dependence modeling and uncertain inputs, Comput. Struct. 142 (2014) 54–63.

[23] Y.C. Bai, X. Han, C. Jiang, and R.G. Bi, A response-surface-based structural reliability analysis method by using non-probability convex model, Appl. Math. Model. 38 (2014) 3834–3847.

[24] E. Jahani, R.L. Muhanna, M.A. Shayanfar and M.A. Barkhordari, Reliability assessment with fuzzy random variables using Interval Monte Carlo Simulation, Comput.-Aided Civil Infrastruct Eng. 29 (2014) 208–220.

[25] C. Jiang, B.Y. Ni, X. Han and Y.R. Tao, Non-probabilistic convex model process: A new method of time-variant uncertainty analysis and its application to structural dynamic reliability problems, Comput. Methods Appl. Mech. Eng. 268 (2014) 656–676.

[26] L. Wang, X. Wang, Y. Li and J. Hu, A non-probabilistic time-variant reliable control method for structural vibration suppression problems with interval uncertainties, Mech. Syst. Signal Process. 115, (2019) 301–322.

[27] M. A. Valdebenito, M. Beer, H. A. Jensen, J. Chen, P. Wei, Fuzzy failure probability estimation applying intervening variables, Struct. Saf. 83 (2020) 101909 (11 pages).

[28] Z. Kang, Y. Luo and A. Li, On non-probabilistic reliability-based design optimization of structures with uncertain-but-bounded parameters, Struct. Saf. 33 (2011) 196–205.

[29] S.-X. Guo and Z.-Z. Lu, A non-probabilistic robust reliability method for analysis and design optimization of structures with uncertain-but-bounded parameters, Appl. Math. Model. 39 (2015) 1985–2002.

[30] P.R. Adduri and R.C. Penmetsa, System reliability analysis for mixed uncertain variables, Struct. Saf. 31 (2009) 375–382.

[31] Y. Luo, Z. Kang and A. Li, Structural reliability assessment based on probability and convex set mixed model, Comput. Struct. 87 (2009) 1408–1415.

[32] J. Wang and Z. Qiu, The reliability analysis of probabilistic and interval hybrid structural system, Appl. Math. Model. 34 (2010) 3648–3658.

[33] U. Alibrandi and C.G. Koh, First-order reliability method for structural reliability analysis in the presence of random and interval variables, ASME J. Risk Uncertainty Part B 1(4) (2015) 041006 (10 pages).

[34] Z. Hu and X. Du, A random field approach to reliability analysis with random and interval variables, ASME J. Risk Uncertainty Part B, 1(4) (2015) 041005 (11 pages).

[35] W. Gao, D. Wu, K. Gao, X. Chen and F. Tin-Loi, Structural reliability analysis with imprecise random and interval fields, Appl. Math. Model. 55 (2018) 49–67.

[36] L.D. Lutes and S. Sarkani, Stochastic Analysis of Structural and Mechanical Vibrations, Prentice-Hall, Upper Saddle River, 1997.

[37] J.B. Roberts, P.D. Spanos, Random vibration and statistical linearization, Dover, 2003.

[38] J. Li and J.B. Chen, Stochastic Dynamics of Structures, John Wiley & Sons, Singapore. 2009.

[39] B. Goller, H.J. Pradlwarter and G.I. Schüeller, Reliability assessment in structural dynamics, J. Sound Vib. 332 (2013) 2488–2499.

[40] S. Gupta and C.S. Manohar, Reliability analysis of randomly vibrating structures with parameter uncertainties, J. Sound Vib. 297 (2006) 1000–1024.

[41] A. Chaudhuri and S. Chakraborty, Reliability of linear structures with parameter uncertainty under non-stationary earthquake, Struct. Saf. 28 (2006) 231–246.

[42] J. Ma, W. Gao, P. Wriggers, T. Wu and S. Sahraee, The analyses of dynamic response and reliability of fuzzy-random truss under stationary stochastic excitation, Comput. Mech. 45 (2010) 443–455.

[43] D.M. Do, W. Gao, C. Song and S. Tangaramvong, Dynamic analysis and reliability assessment of structures with uncertain-but-bounded parameters under stochastic process excitations, Reliab. Eng. Syst. Safe. 132 (2014) 46–59.

[44] G. Muscolino, R. Santoro and A. Sofi, Explicit reliability sensitivities of linear structures with interval uncertainties under stationary stochastic excitations, Struct. Saf., 52, Part B, (2015) 219–232.

[45] G. Muscolino, R. Santoro and A. Sofi, Reliability analysis of structures with interval uncertainties under stationary stochastic excitations, Comput. Methods Appl. Mech. Eng. 300 (2016) 47–69.

[46] G. Muscolino, R. Santoro and A. Sofi, Interval fractile levels for stationary stochastic response of linear structures with uncertainties, ASME J. Risk Uncertainty Part B 2(1) (2016) 011004 (11 pages).

[47] S. Ferson, V. Kreinovich, L. Ginzburg, D.S. Myers, K. Sentz, Constructing probability boxes and Dempster-Shafer structures, Sandia National Laboratories SAND2002–4015 (2003).

[48] G. Muscolino and A. Sofi, Bounds for the stationary stochastic response of truss structures with uncertain-but-bounded parameters, Mech. Syst. Signal Process. 37 (2013) 163-181.

[49] G. Muscolino and A. Sofi, Stochastic analysis of structures with uncertain-but-bounded parameters via improved interval analysis, Probab. Eng. Mech. 28 (2012) 152-163.

[50] A. Sofi, G. Muscolino, F. Giunta, A sensitivity-based approach for reliability analysis of randomly excited structures with interval axial stiffness, ASME J. Risk Uncertainty Part B, 6 (2020) 041008 (10 pages).

[51] M.G.R. Faes, M. A. Valdebenito,D. Moens, M. Beer, Bounding the first excursion probability of linear structures subjected to imprecise stochastic loading, Comput. Struct. 239 (2020), Article number 106320 (14 pages).

[52] R. Santoro, A. Sofi, A., F. Tubino, Serviceability Assessment of Footbridges via Improved Interval Analysis, ASME J. Risk Uncertainty Part B (2021) doi: https://doi.org/10.1115/1.4050169

[53] W. Verhaeghe, W. Desmet, D. Vandepitte, D. Moens, Interval fields to represent uncertainty on the output side of a static FE analysis, Comput. Methods Appl. Mech. Eng. 260 (2013) 50-62.

[54] A. Sofi, E. Romeo, O. Barrera, A. Cocks An interval finite element method for the analysis of structures with spatially varying uncertainties, Adv. Eng. Softw. 128 (2019), 1-19.

[55] A. Sofi and E. Romeo, A novel Interval Finite Element Method based on the improved interval analysis, Comput. Methods Appl. Mech. Eng. 311 (2016) 671–697.

[56] A. E. Mansour, An Introduction to Structural Reliability Theory, Ship Structure Committee, SSC-351 Report, 1990.

[57] A. Pownuk, L. Longpré, V. Kreinovich, Checking monotonicity is NP-hard even for cubic polynomials, Reliable Comput. 18 (2013) 90-96.

[58] S. H. Crandall, K. L. Chandiramani, R. G. Cook, Some First-Passage Problems in Random Vibration, J. Applied Mechanics (ASME) 33 (1966) 532-538.

[59] E. Simiu and R. Scanlan, Wind Effects on Structures, John Wiley & Sons, New York, 1996.

[60] A.G. Davenport, The spectrum of horizontal gustiness near the ground in high winds, Q. J. Roy. Meteorol. Soc. 87 (1961) 194–211.

[61] W. Dong, H. Shah, Vertex method for computing functions of fuzzy variables, Fuzzy Sets Syst. 24 (1987) 65–78.

## Figure captions

**Figure 1.** Flowchart of the proposed sensitivity-based procedure for interval reliability analysis.

**Figure 2.** Steel telecommunication antenna mast under wind excitation: a) 2D model; b) FE discretization.

**Figure 3.** *UB* and *LB* of the a) *interval CDF* and b) *interval failure probability* (semi-logarithmic scale) of the *extreme value* axial stress process $Y_{1,\max}^{(1)I}(T)$ of the telecommunication antenna with uncertain Young's moduli $E^{(i)I} = E_0\left(1+\Delta\alpha\hat{e}_{(\mathrm{K})i}^{I}\right)$, $(i=1,2,\ldots,r_{\mathrm{K}}=12)$: comparison between the proposed procedure, the *vertex method* ($\Delta\alpha=0.10$) and the nominal solution.

**Figure 4.** *UB* and *LB* of the a) *interval CDF* and b) *interval failure probability* (semi-logarithmic scale) of the *extreme value* axial stress process $Y_{1,\max}^{(1)I}(T)$ of the telecommunication antenna with uncertain Young's moduli $E^{(i)I} = E_0\left(1+\Delta\alpha\hat{e}_{(\mathrm{K})i}^{I}\right)$, $(i=1,2,\ldots,r_{\mathrm{K}}=12)$: comparison between the proposed procedure, the *vertex method* ($\Delta\alpha=0.20$) and the nominal solution.

**Figure 5**. *Functions of sensitivity* of the *interval reliability function* of the *extreme value* axial stress process $Y_{1,\max}^{(1)I}(T)$ of the telecommunication antenna with respect to the fluctuations of Young's moduli $E^{(i)I} = E_0\left(1+\Delta\alpha\hat{e}_{(\mathrm{K})i}^{I}\right)$, $(i=1,2,\ldots,8,12,13,14,16,17)$, versus the deterministic barrier level $b$ ($\Delta\alpha=0.10$, $T=1000T_0$).

**Figure 6**. *Functions of sensitivity* of the *interval reliability function* of the *extreme value* axial stress process $Y_{1,\max}^{(1)I}(T)$ with respect to the fluctuations of Young's moduli $E^{(i)I} = E_0\left(1+\Delta\alpha\hat{e}_{(\mathrm{K})i}^{I}\right)$, $(i=1,2,\ldots,19)$, evaluated for the barrier level $b$ having a probability $p=0.50$ of not being exceeded ($\Delta\alpha=0.10$, $T=1000T_0$).

**Figure 7**. *UB* and *LB* of the *interval CDF* of the *extreme value* axial stress process $Y_{1,\max}^{I}(T)$ $Y_{1,\max}^{(1)I}(T)$ of the telecommunication antenna provided by the proposed procedure considering Young's moduli of all the 19 FEs as uncertain (full) and retaining only the first $r_{\mathrm{K}}=6$ and $r_{\mathrm{K}}=13$ most influential uncertain parameters (reduced): a) $\Delta\alpha=0.10$ and b) $\Delta\alpha=0.20$ ($T=1000T_0$).

**Figure** 8. *UB* and *LB* of the *interval fractiles* of order a) $p=0.50$ and b) $p=0.95$ ($T=1000T_0$) of the *extreme value* axial stress process $Y_{1,\max}^{(1)I}(T)$ of the telecommunication antenna provided by the proposed procedure and the *vertex method* versus the deviation amplitude $\Delta\alpha$ of the interval Young's moduli $E^{(i)I}=E_0\left(1+\Delta\alpha\hat{e}_{(\mathrm{K})i}^{I}\right)$, $(i=1,2,\ldots,r_{\mathrm{K}}=12)$.

**Figure 9.** Ten-story shear-type frame under wind excitation.

**Figure 10**. *Functions of sensitivity* of the *interval reliability function* of the *extreme value* shear stress process $Y_{2,\max}^{(2)I}(T)$ of the frame structure with respect to the fluctuations of a) Young's moduli $E^{(i)I}=E_0\left(1+\Delta\alpha\hat{e}_{(\mathrm{K})i}^{I}\right)$, $(i=1,2,\ldots,r_{\mathrm{K}}=10)$, and of b) floor masses $m^{(i)I}=m_0\left(1+\Delta\alpha\hat{e}_{(\mathrm{M})i}^{I}\right)$, $(i=1,2,\ldots,r_{\mathrm{M}}=10)$, versus the deterministic barrier level $b$ ($\Delta\alpha=0.10$, $T=1000T_0$).

**Figure 11**. *Functions of sensitivity* of the *interval reliability function* of the *extreme value* shear stress process $Y_{2,\max}^{(2)I}(T)$ of the frame structure with respect to the fluctuations of a) Young's moduli $E^{(i)I}=E_0\left(1+\Delta\alpha\hat{e}_{(\mathrm{K})i}^{I}\right)$, $(i=1,2,\ldots,r_{\mathrm{K}}=10)$, and of b) floor masses $m^{(i)I}=m_0\left(1+\Delta\alpha\hat{e}_{(\mathrm{M})i}^{I}\right)$, $(i=1,2,\ldots,r_{\mathrm{M}}=10)$, evaluated for the barrier level $b$ having a probability $p=0.50$ of not being exceeded ($\Delta\alpha=0.10$, $T=1000T_0$).

**Figure 12.** Zero-order spectral moment of the shear stress random process $Y_2^{(2)}(t)$: a) comparison between the nominal spectral moment and the one evaluated assuming all the uncertain parameters equal to the nominal values except the *i*-th Young's modulus which is set equal to its *UB* i.e. $E^{(i)} = E_0\left(1+\Delta\alpha\right),\ (i=1,2,\ldots,10)$ for $\Delta\alpha = 0.10$; b) enlargement for $i \geq 2$.

**Figure 13.** Zero-order spectral moment of the shear stress random process $Y_2^{(2)}(t)$: comparison between the nominal spectral moment and the one evaluated assuming all the uncertain parameters equal to the nominal values except the mass of the *i*-th floor which is set equal to its *UB* i.e. $m^{(i)} = m_0\left(1+\Delta\alpha\right),\ (i=1,2,\ldots,10)$ for $\Delta\alpha = 0.10$.

**Figure 14.** *UB* and *LB* of the a) *interval CDF* and b) *interval failure probability* of the *extreme value* shear stress process $Y_{2,\max}^{(2)I}(T)$ of the frame structure with uncertain Young's moduli $E^{(i)I} = E_0\left(1+\Delta\alpha\hat{e}_{(\mathrm{K})i}^{I}\right),\quad (i=1,2,3,4,5,10)$, and floor masses $m^{(i)I} = m_0\left(1+\Delta\alpha\hat{e}_{(\mathrm{M})i}^{I}\right)$, $(i=1,2,3,4,9,10)$: comparison between the proposed procedure, the *vertex method* $(\Delta\alpha = 0.10)$ and the nominal solution.

**Figure 15.** *UB* and *LB* of the a) *interval CDF* and b) *interval failure probability* of the *extreme value* shear stress process $Y_{2,\max}^{(2)I}(T)$ of the frame structure with uncertain Young's moduli $E^{(i)I} = E_0\left(1+\Delta\alpha\hat{e}_{(\mathrm{K})i}^{I}\right),\quad (i=1,2,3,4,5,10)$, and floor masses $m^{(i)I} = m_0\left(1+\Delta\alpha\hat{e}_{(\mathrm{M})i}^{I}\right)$, $(i=1,2,3,4,9,10)$: comparison between the proposed procedure, the *vertex method* $(\Delta\alpha = 0.20)$ and the nominal solution.

**Figure 16**. *UB* and *LB* of the *interval fractiles* of order $p = 0.50$ a) and b) $p = 0.95$ $(T = 1000T_0)$ of the *extreme value* shear stress process $Y_{2,\max}^{(2)I}(T)$ of the frame structure provided by the proposed procedure and the *vertex method* versus the deviation amplitude $\Delta\alpha$ of the interval Young's moduli $E^{(i)I} = E_0\left(1+\Delta\alpha\hat{e}_{(\mathrm{K})i}^{I}\right),\ (i=1,2,3,4,5,10)$, and floor masses $m^{(i)I} = m_0\left(1+\Delta\alpha\hat{e}_{(\mathrm{M})i}^{I}\right)$, $(i=1,2,3,4,9,10)$.

**Figure 17.** *UB* and *LB* of the *interval CDF* of the *extreme value* shear stress process $Y_{2,\max}^{(2)I}(T)$ of the frame structure provided by the proposed procedure considering all Young's moduli and floor masses as uncertain (full) and retaining only the first $r_K = r_M = 6$ and $r_K = r_M = 7$ most influential uncertain parameters (reduced): *a*) $\Delta\alpha = 0.10$ and *b*) $\Delta\alpha = 0.20$ ($T = 1000T_0$).

## Table captions

**Table 1.** Properties of the telecommunication antenna mast.

**Table 2.** Cross-section of the columns of the frame structure.

**Credit Author Statement**

**Alba Sofi:** Conceptualization, Methodology, Writing-Original draft preparation, Writing - Review & Editing, Validation, Visualization, Supervision. **Filippo Giunta:** Software, Validation, Visualization. **Giuseppe Muscolino:** Conceptualization, Methodology, Writing - Review & Editing, Supervision

**Declaration of interests**

☒ The authors declare that they have no known competing financial interests or personal relationships that could have appeared to influence the work reported in this paper.

☐The authors declare the following financial interests/personal relationships which may be considered as potential competing interests:

| |
|---|
| |

**Table 1.** Properties of the telecommunication antenna mast.

| Node | Height [m] | Outer diameter [m] | Thickness [m] | Lumped mass [t] | Tributary area [$m^2$] |
|---|---|---|---|---|---|
| 2 | 1.50 | 0.9148 | 0.008 | 0.3050 | 1.3722 |
| 3 | 3.00 | 0.9148 | 0.008 | 0.3050 | 1.3722 |
| 4 | 4.50 | 0.9148 | 0.008 | 0.2754 | 1.2957 |
| 5 | 6.00 | 0.8128 | 0.0071 | 0.2458 | 1.2192 |
| 6 | 7.50 | 0.8128 | 0.0071 | 0.2458 | 1.2192 |
| 7 | 9.00 | 0.8128 | 0.0071 | 0.2211 | 1.143 |
| 8 | 10.50 | 0.7112 | 0.0063 | 0.1964 | 1.0668 |
| 9 | 12.00 | 0.7112 | 0.0063 | 0.1964 | 1.066 |
| 10 | 13.50 | 0.7112 | 0.0063 | 0.1760 | 0.9906 |
| 11 | 15.00 | 0.6096 | 0.0056 | 0.1530 | 0.9144 |
| 12 | 16.50 | 0.6096 | 0.0056 | 0.1505 | 0.9144 |
| 13 | 18.00 | 0.6096 | 0.0056 | 0.1288 | 0.8382 |
| 14 | 19.50 | 0.508 | 0.005 | 0.2671 | 0.762 |
| 15 | 21.00 | 0.508 | 0.005 | 0.1071 | 0.762 |
| 16 | 22.50 | 0.508 | 0.005 | 0.1650 | 0.526275 |
| 17 | 24.00 | 0.1937 | 0.0045 | 0.0429 | 0.29055 |
| 18 | 25.50 | 0.1937 | 0.0045 | 0.1329 | 0.29055 |
| 19 | 27.00 | 0.1937 | 0.0045 | 0.0429 | 0.29055 |
| 20 | 28.50 | 0.1937 | 0.0045 | 0.0214 | 0.145275 |

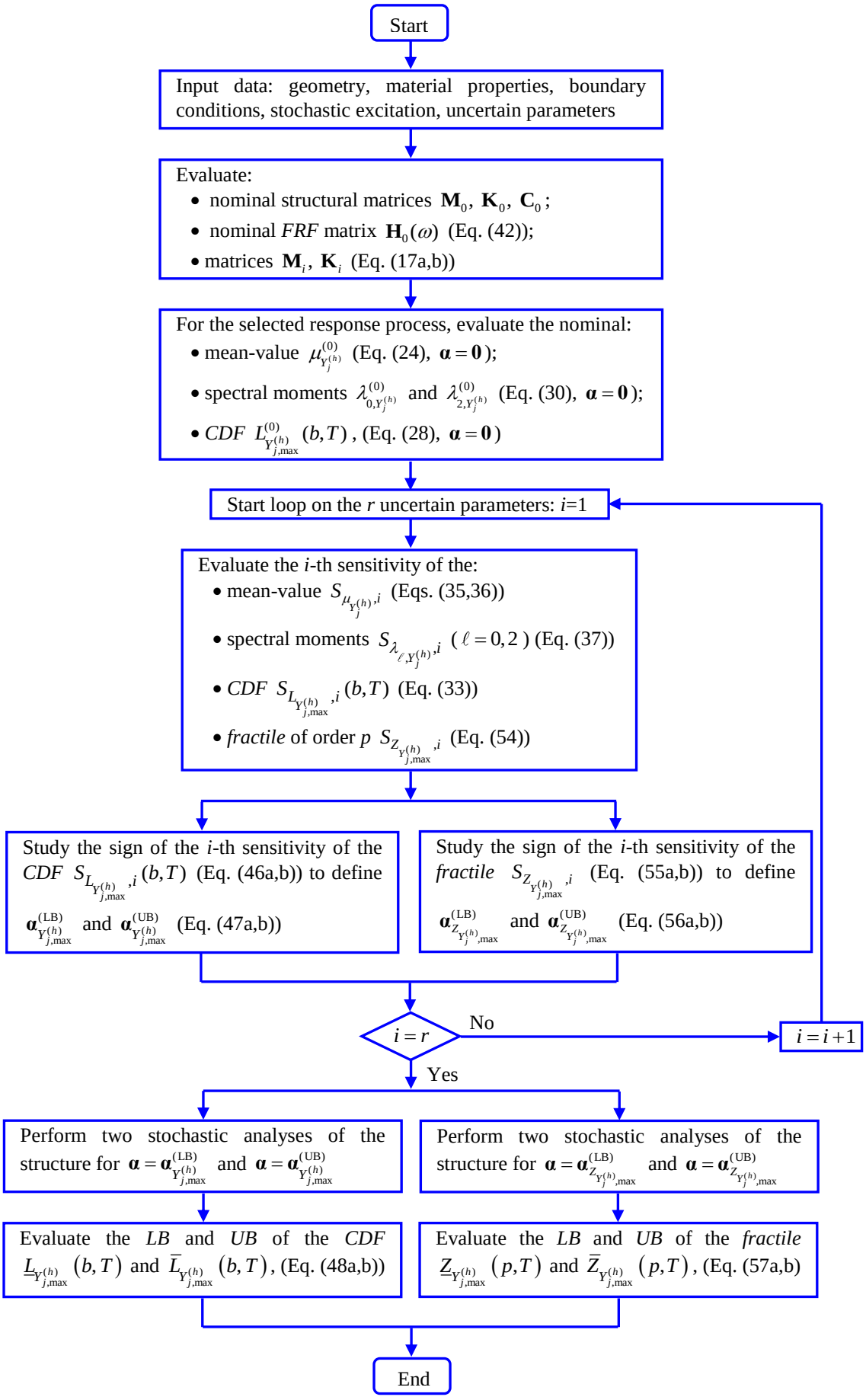


**Figure 1.** Flowchart of the proposed sensitivity-based procedure for interval reliability analysis.

**Figure 2**

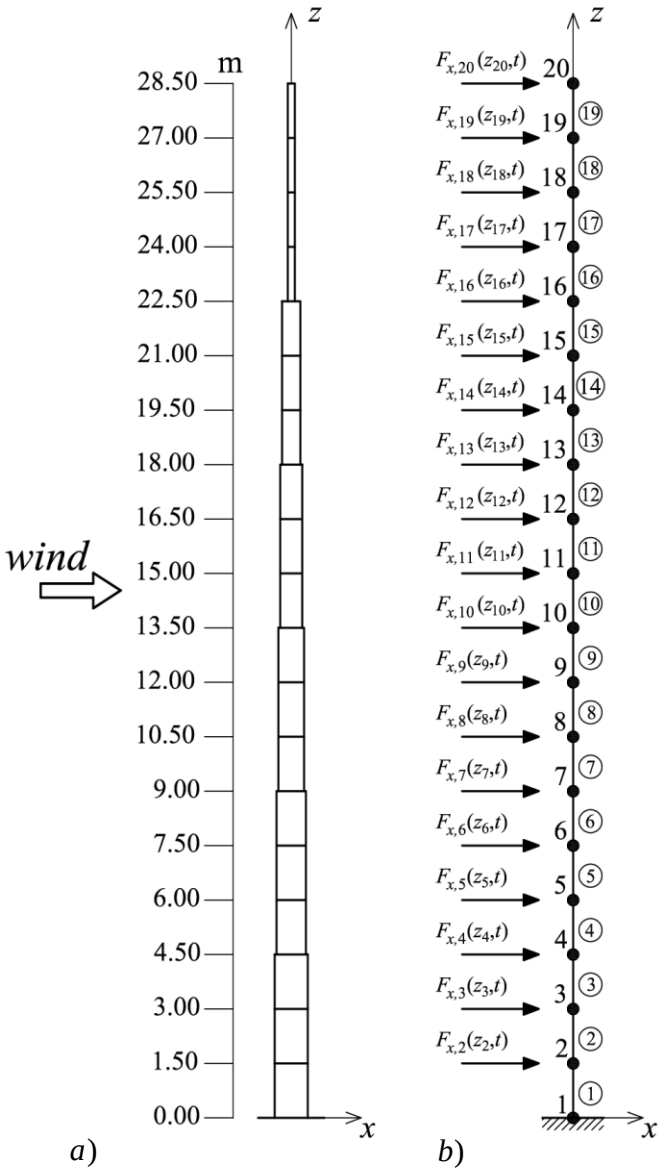


**Figure 2.** Steel telecommunication antenna mast under wind excitation: a) 2D model; b) FE discretization.

**Figure 3**

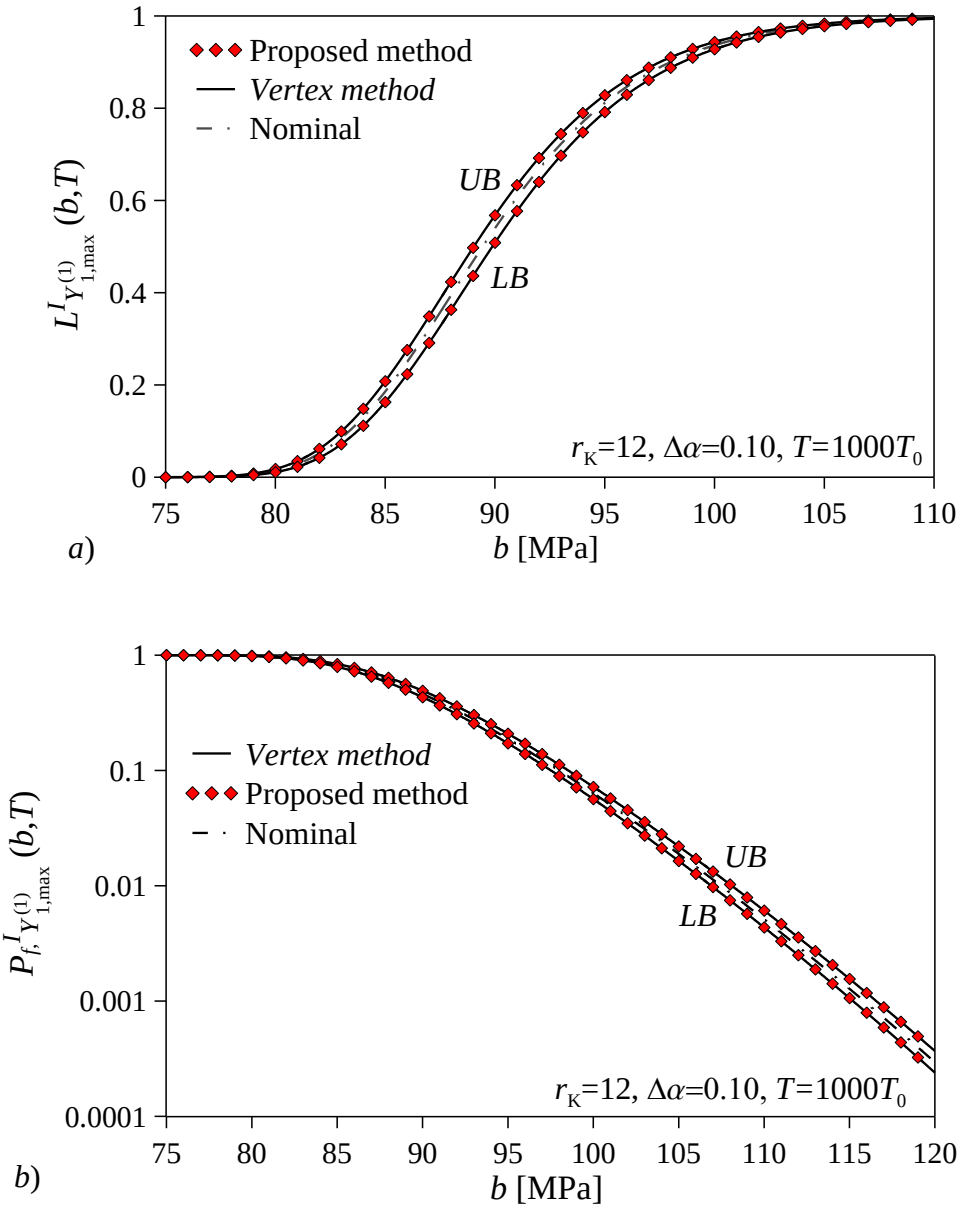


**Figure 3.** *UB* and *LB* of the a) *interval CDF* and b) *interval failure probability* (semi-logarithmic scale) of the *extreme value* axial stress process $Y^{(1)I}_{1,\max}(T)$ of the telecommunication antenna with uncertain Young's moduli $E^{(i)I} = E_0\left(1+\Delta\alpha\hat{e}^I_{(K)i}\right)$, $(i=1,2,\ldots,r_K=12)$: comparison between the proposed procedure, the *vertex method* ($\Delta\alpha=0.10$) and the nominal solution.

**Figure 4**

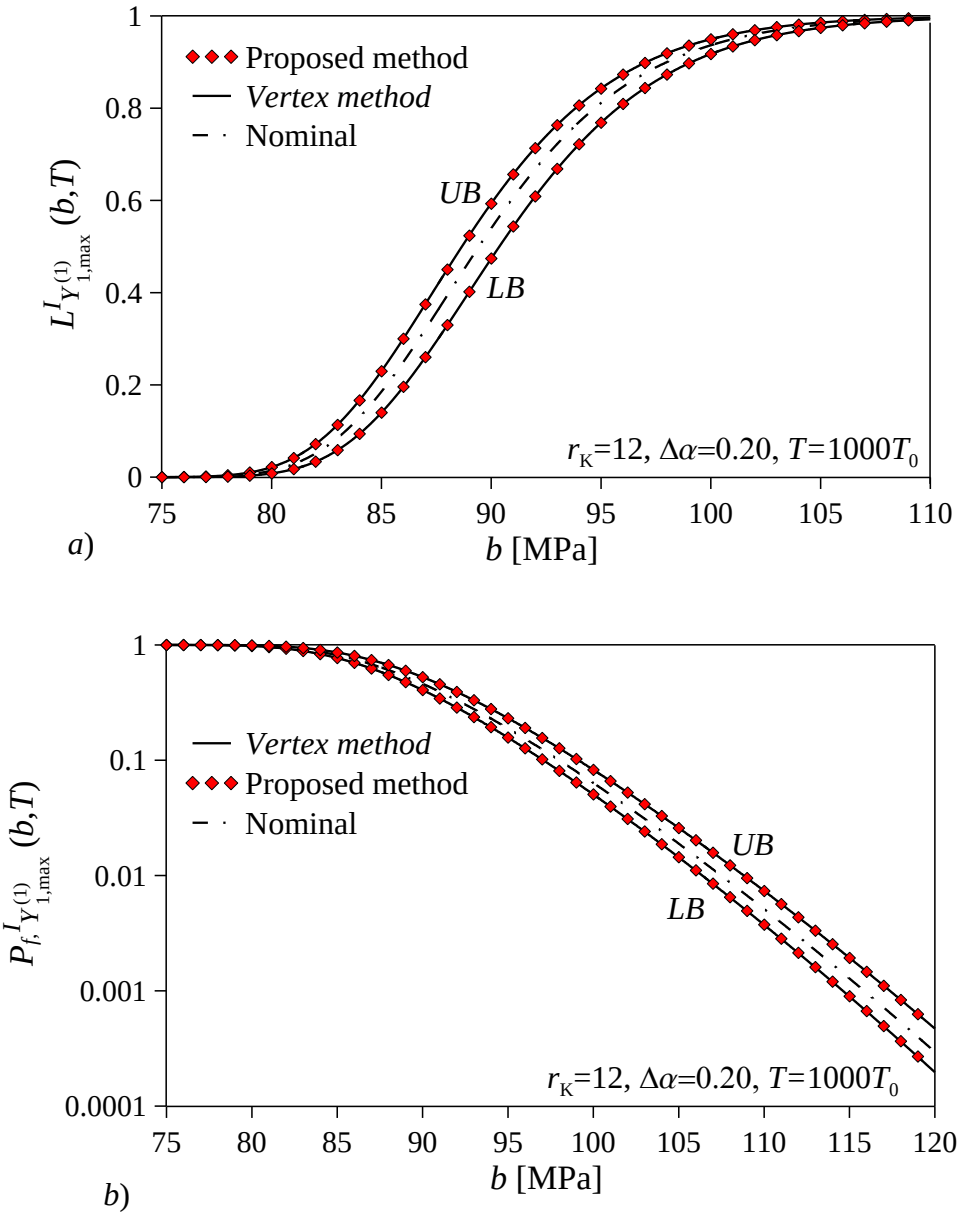


**Figure 4.** *UB* and *LB* of the a) *interval CDF* and b) *interval failure probability* (semi-logarithmic scale) of the *extreme value* axial stress process $Y^{(1)I}_{1,\max}(T)$ of the telecommunication antenna with uncertain Young's moduli $E^{(i)I} = E_0\left(1+\Delta\alpha\hat{e}^I_{(K)i}\right)$, $(i=1,2,\ldots,r_K=12)$: comparison between the proposed procedure, the *vertex method* ($\Delta\alpha=0.20$) and the nominal solution.

**Figure 5**

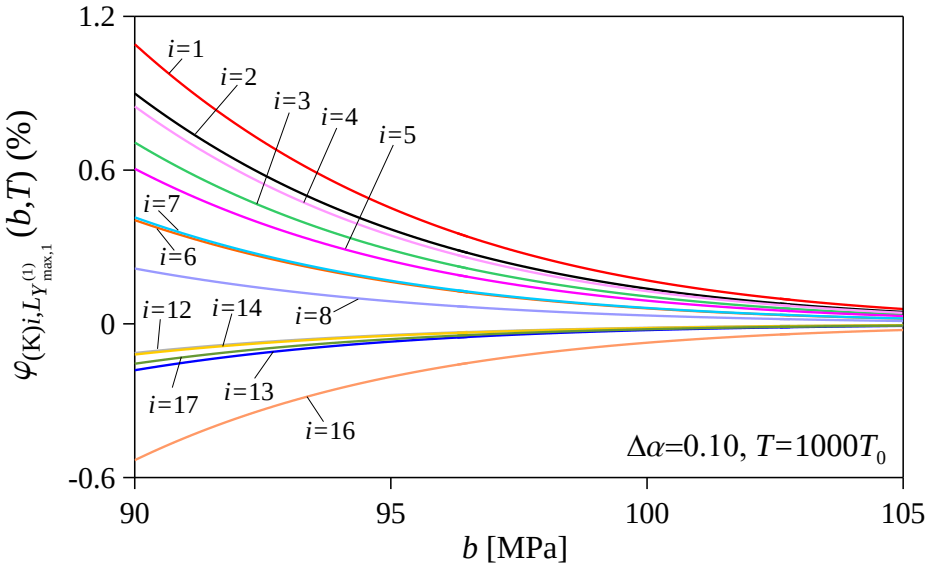


**Figure 5**. *Functions of sensitivity* of the *interval reliability function* of the *extreme value* axial stress process $Y_{1,\max}^{(1)I}(T)$ of the telecommunication antenna with respect to the fluctuations of Young's moduli $E^{(i)I} = E_0\left(1+\Delta\alpha\hat{e}_{(\mathrm{K})i}^{I}\right)$, $(i=1,2,\ldots,8,12,13,14,16,17)$, versus the deterministic barrier level $b$ $(\Delta\alpha=0.10,\, T=1000T_0)$.

**Figure 6**

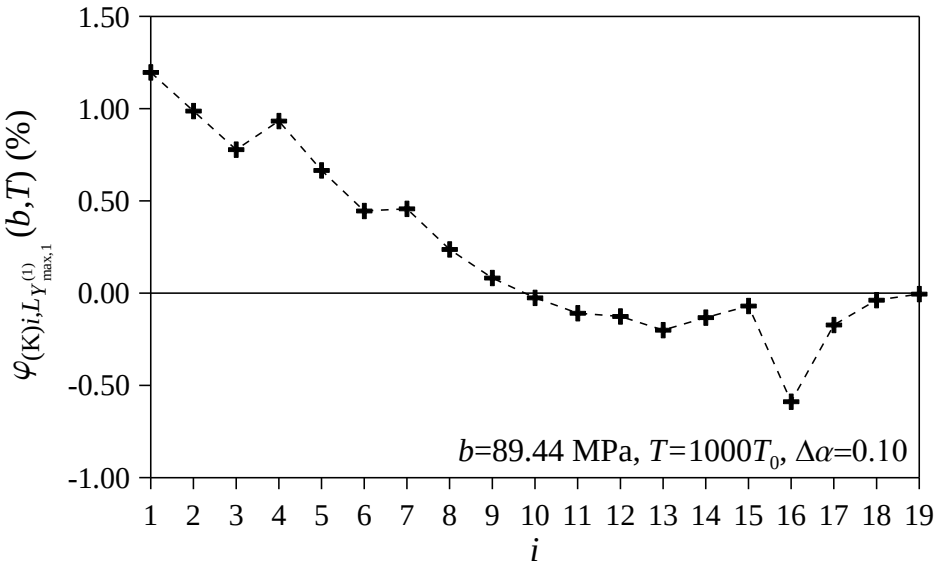


**Figure 6**. *Functions of sensitivity* of the *interval reliability function* of the *extreme value* axial stress process $Y^{(1)I}_{1,\max}(T)$ with respect to the fluctuations of Young's moduli $E^{(i)I} = E_0\left(1+\Delta\alpha\hat{e}^I_{(K)i}\right)$, $(i=1,2,\ldots,19)$, evaluated for the barrier level $b$ having a probability $p=0.50$ of not being exceeded $(\Delta\alpha=0.10,\ T=1000T_0)$.

**Figure 7**

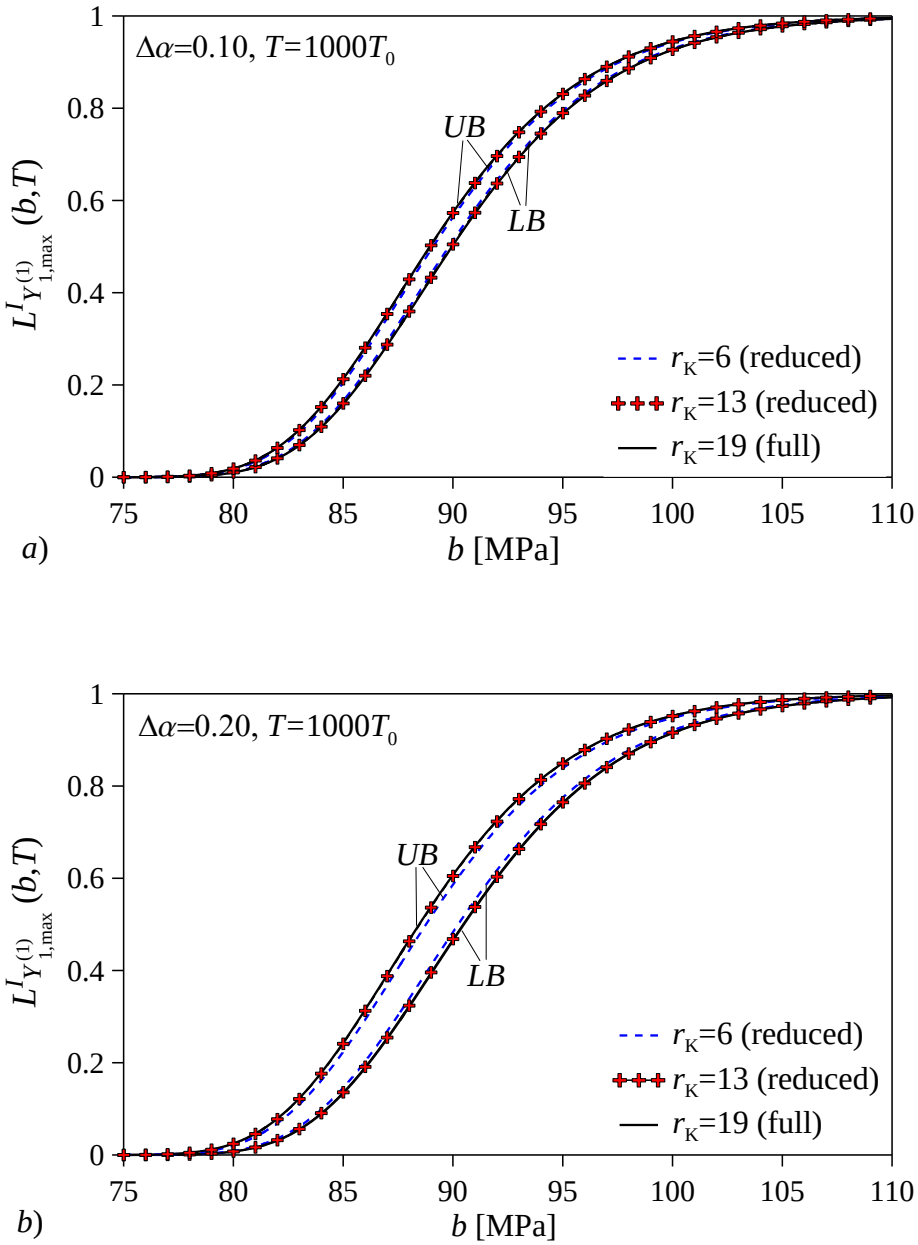


**Figure 7**. *UB* and *LB* of the *interval CDF* of the *extreme value* axial stress process $Y^{I}_{1,\max}(T)$ $Y^{(1)I}_{1,\max}(T)$ of the telecommunication antenna provided by the proposed procedure considering Young's moduli of all the 19 FEs as uncertain (full) and retaining only the first $r_K = 6$ and $r_K = 13$ most influential uncertain parameters (reduced): a) $\Delta\alpha = 0.10$ and b) $\Delta\alpha = 0.20$ ($T = 1000T_0$).

**Figure 8**

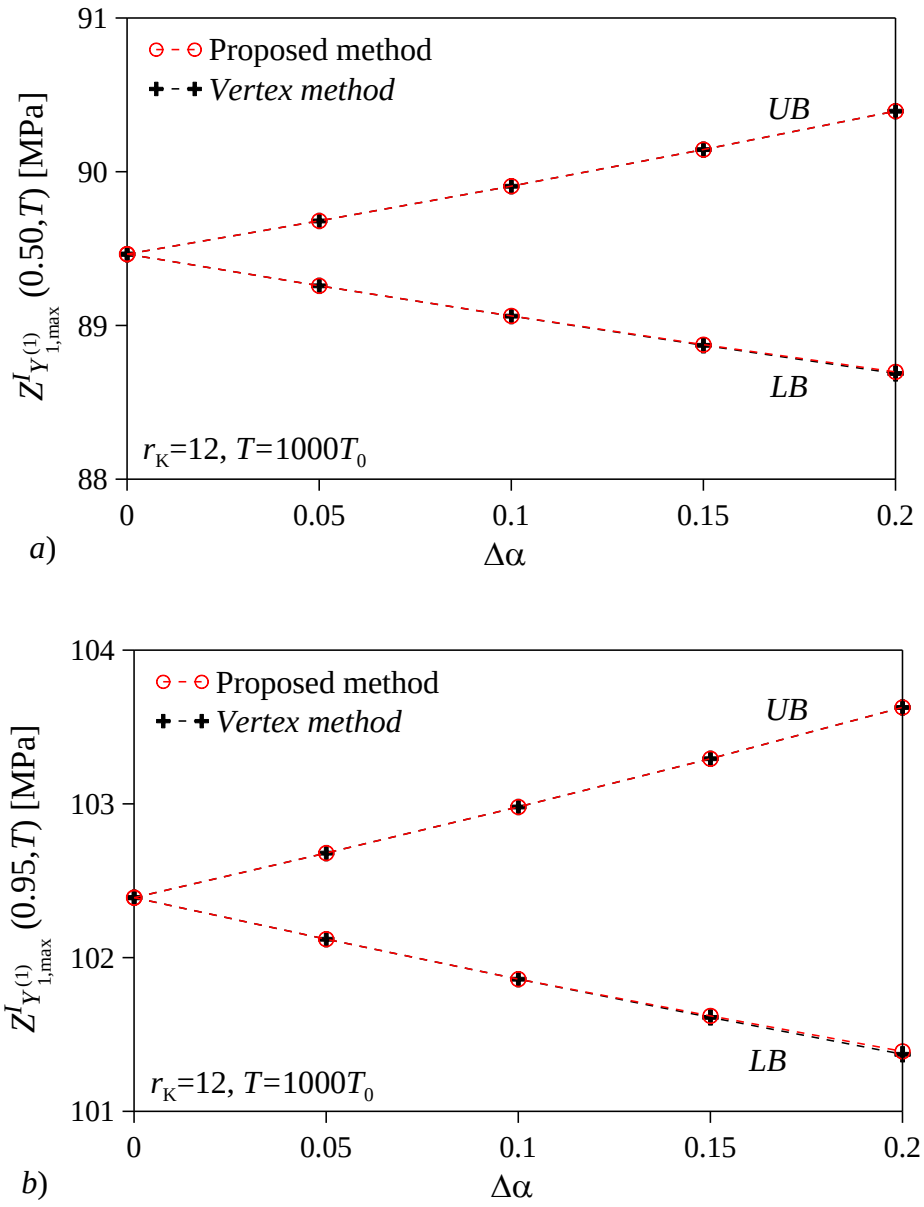


**Figure 8**. *UB* and *LB* of the *interval fractiles* of order a) $p=0.50$ and b) $p=0.95$ ($T=1000T_0$) of the *extreme value* axial stress process $Y^{(1)I}_{1,\max}(T)$ of the telecommunication antenna provided by the proposed procedure and the *vertex method* versus the deviation amplitude $\Delta\alpha$ of the interval Young's moduli $E^{(i)I}=E_0\left(1+\Delta\alpha\hat{e}^I_{(K)i}\right)$, $(i=1,2,\ldots,r_K=12)$.

**Figure 9**

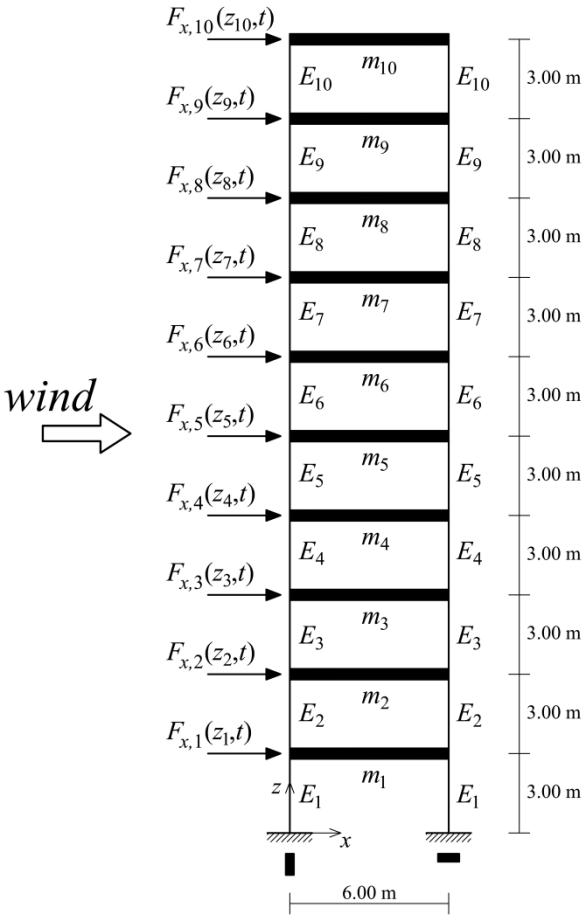


**Figure 9.** Ten-story shear-type frame under wind excitation.

**Figure 10**

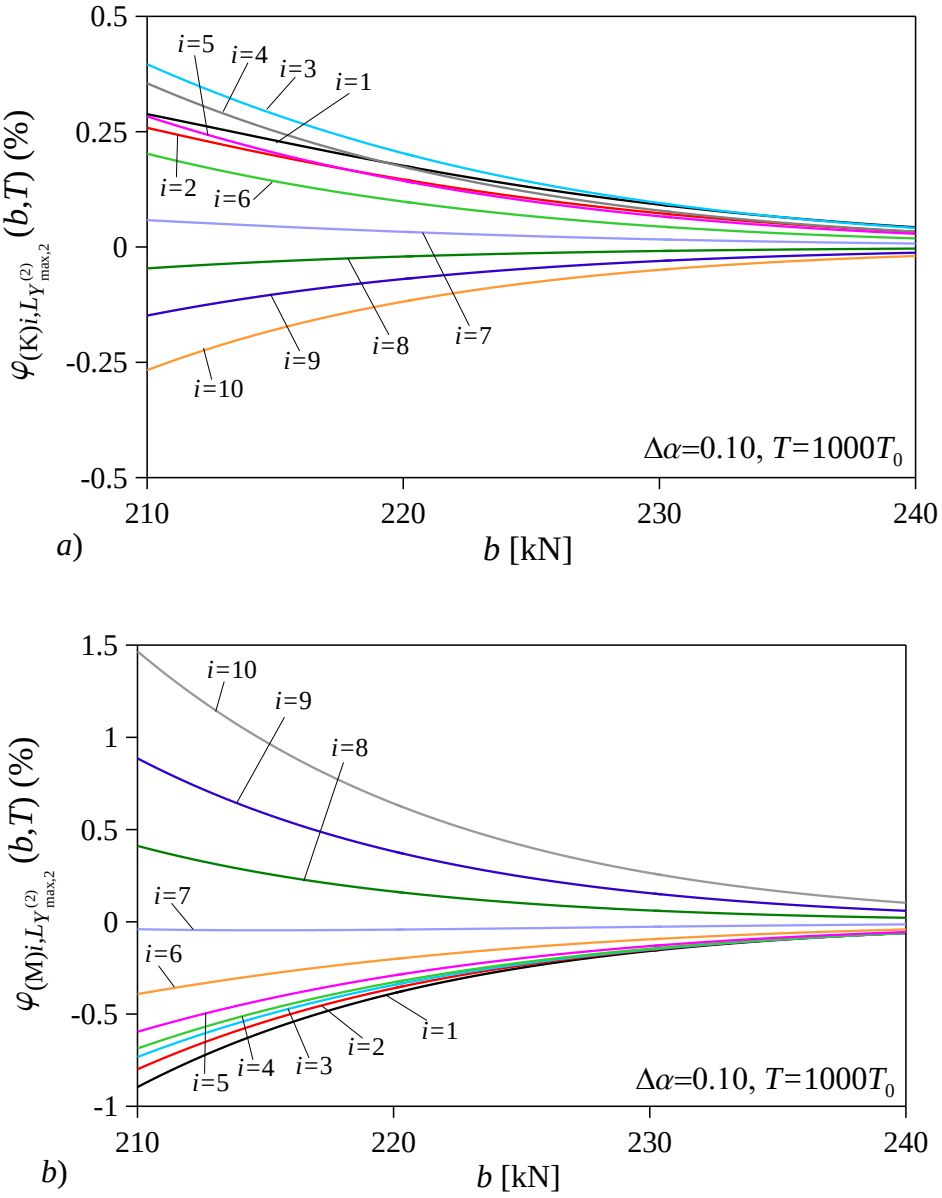


**Figure 10**. *Functions of sensitivity* of the *interval reliability function* of the *extreme value* shear stress process $Y^{(2)I}_{2,\max}(T)$ of the frame structure with respect to the fluctuations of a) Young's moduli $E^{(i)I} = E_0\left(1+\Delta\alpha\hat{e}^I_{(K)i}\right)$, $(i=1,2,\ldots,r_K=10)$, and of b) floor masses $m^{(i)I} = m_0\left(1+\Delta\alpha\hat{e}^I_{(M)i}\right)$, $(i=1,2,\ldots,r_M=10)$, versus the deterministic barrier level $b$ $(\Delta\alpha=0.10,\, T=1000T_0)$.

**Figure 11**

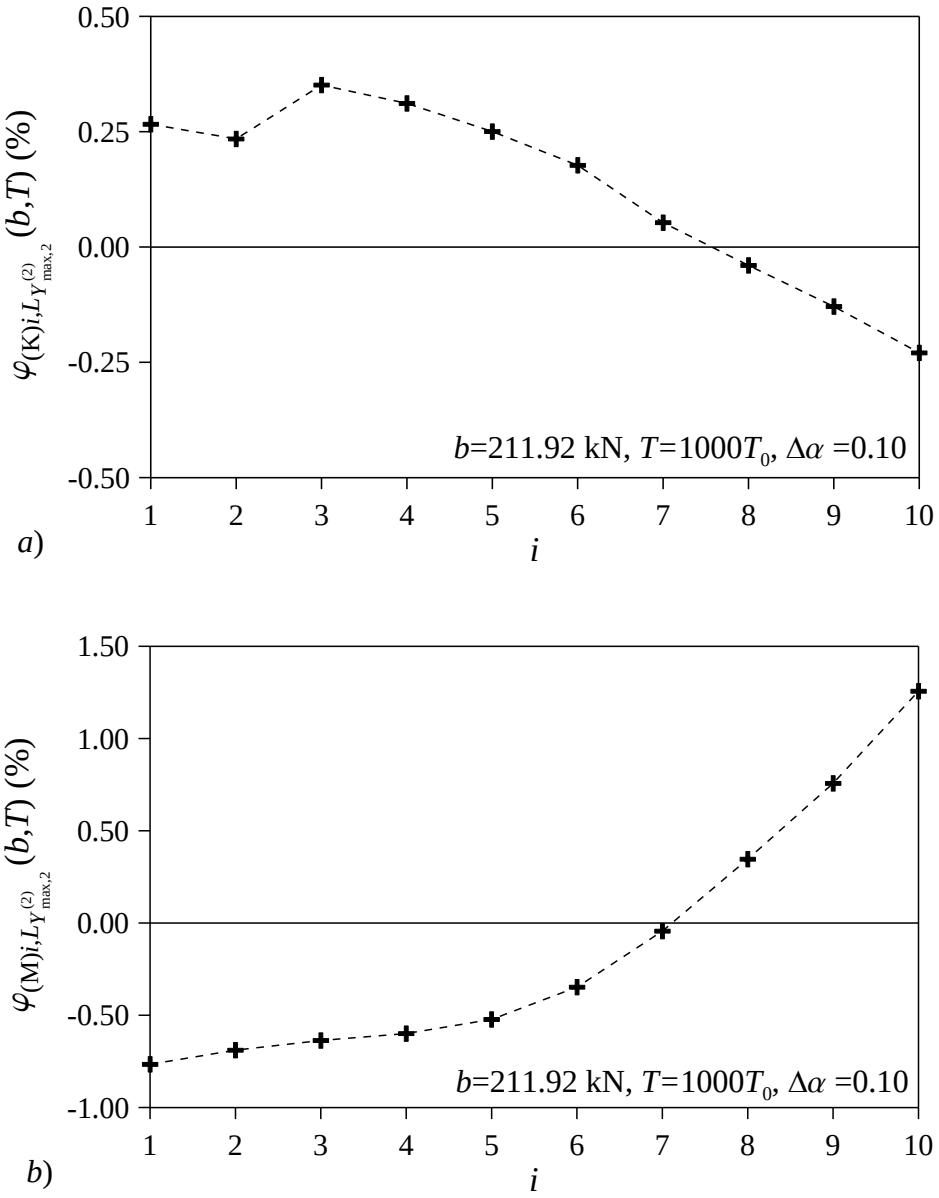


**Figure 11**. *Functions of sensitivity* of the *interval reliability function* of the *extreme value* shear stress process $Y_{2,\max}^{(2)I}(T)$ of the frame structure with respect to the fluctuations of a) Young's moduli $E^{(i)I} = E_0\left(1+\Delta\alpha\hat{e}_{(\mathrm{K})i}^{I}\right)$, $(i=1,2,\ldots,r_{\mathrm{K}}=10)$, and of b) floor masses $m^{(i)I} = m_0\left(1+\Delta\alpha\hat{e}_{(\mathrm{M})i}^{I}\right)$, $(i=1,2,\ldots,r_{\mathrm{M}}=10)$, evaluated for the barrier level $b$ having a probability $p=0.50$ of not being exceeded ($\Delta\alpha=0.10$, $T=1000T_0$).

**Figure 12**

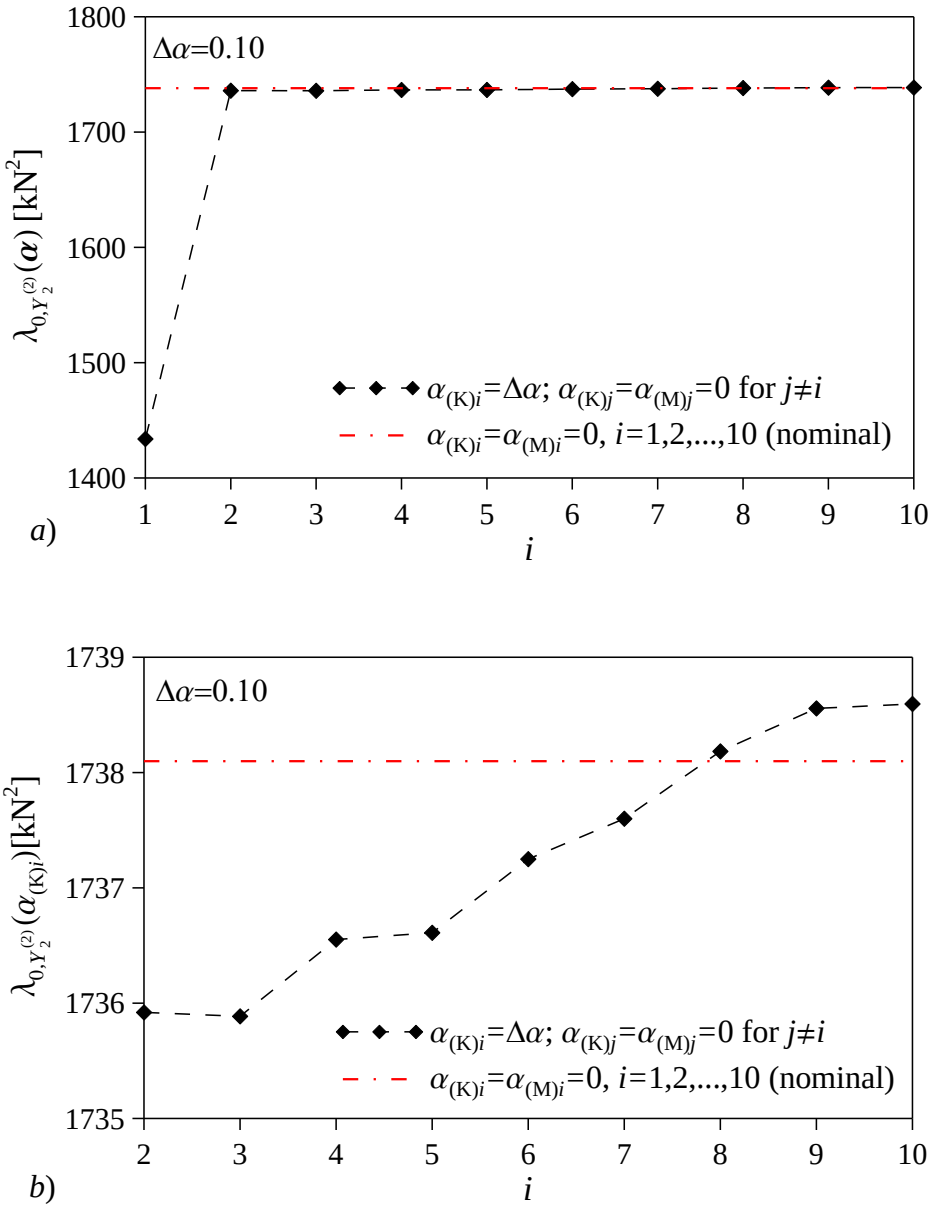


**Figure 12.** Zero-order spectral moment of the shear stress random process $Y_2^{(2)}(t)$: a) comparison between the nominal spectral moment and the one evaluated assuming all the uncertain parameters equal to the nominal values except the *i*-th Young's modulus which is set equal to its *UB* i.e. $E^{(i)} = E_0\left(1+\Delta\alpha\right)$, $(i=1,2,\ldots,10)$ for $\Delta\alpha = 0.10$; b) enlargement for $i \geq 2$.

**Figure 13**

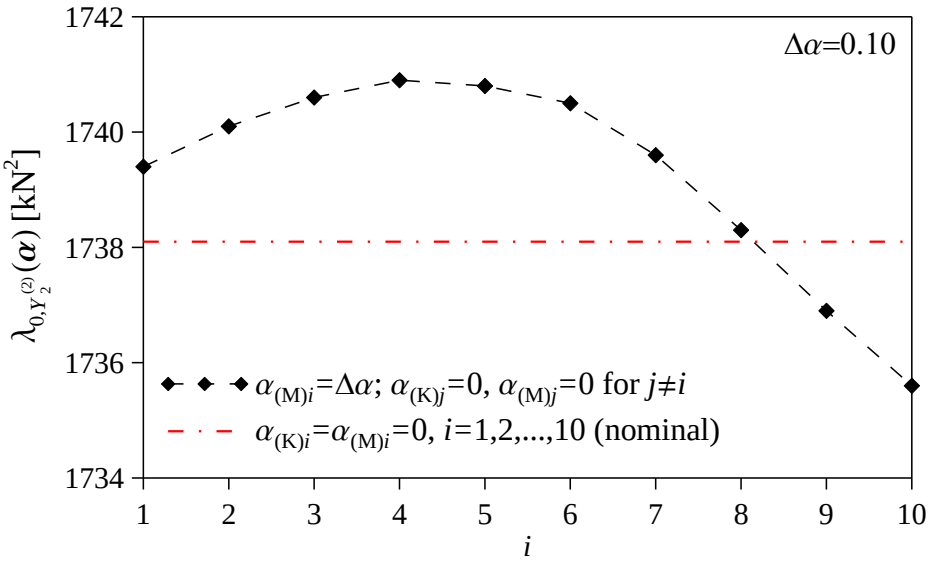


**Figure 13.** Zero-order spectral moment of the shear stress random process $Y_2^{(2)}(t)$: comparison between the nominal spectral moment and the one evaluated assuming all the uncertain parameters equal to the nominal values except the mass of the *i*-th floor which is set equal to its *UB* i.e. $m^{(i)} = m_0\left(1+\Delta\alpha\right),\ (i=1,2,\ldots,10)$ for $\Delta\alpha = 0.10$.

**Figure 14**

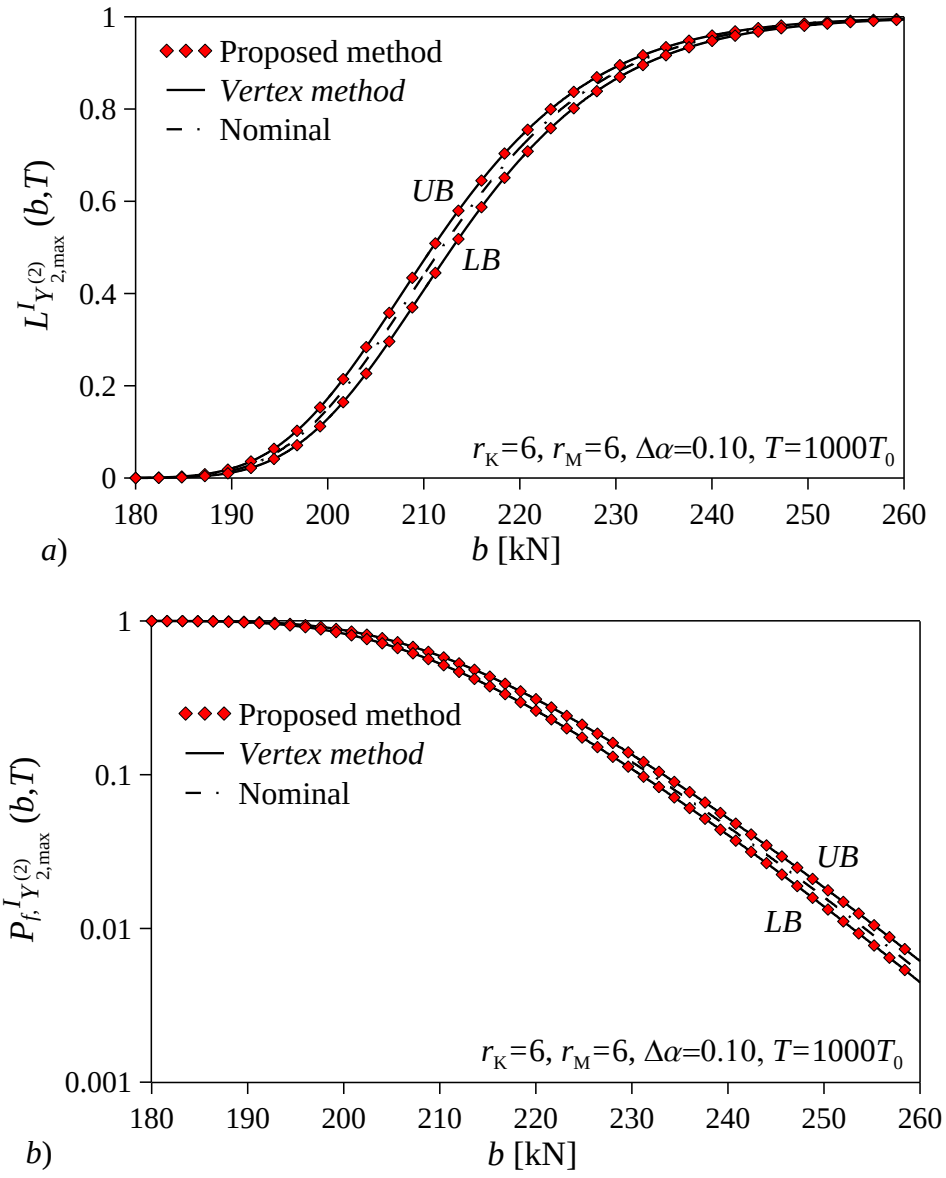


**Figure 14.** *UB* and *LB* of the a) *interval CDF* and b) *interval failure probability* of the *extreme value* shear stress process $Y^{(2)I}_{2,\max}(T)$ of the frame structure with uncertain Young's moduli $E^{(i)I} = E_0\left(1+\Delta\alpha\hat{e}^I_{(\mathrm{K})i}\right)$, $(i=1,2,3,4,5,10)$, and floor masses $m^{(i)I} = m_0\left(1+\Delta\alpha\hat{e}^I_{(\mathrm{M})i}\right)$, $(i=1,2,3,4,9,10)$: comparison between the proposed procedure, the *vertex method* $(\Delta\alpha=0.10)$ and the nominal solution.

**Figure 15**

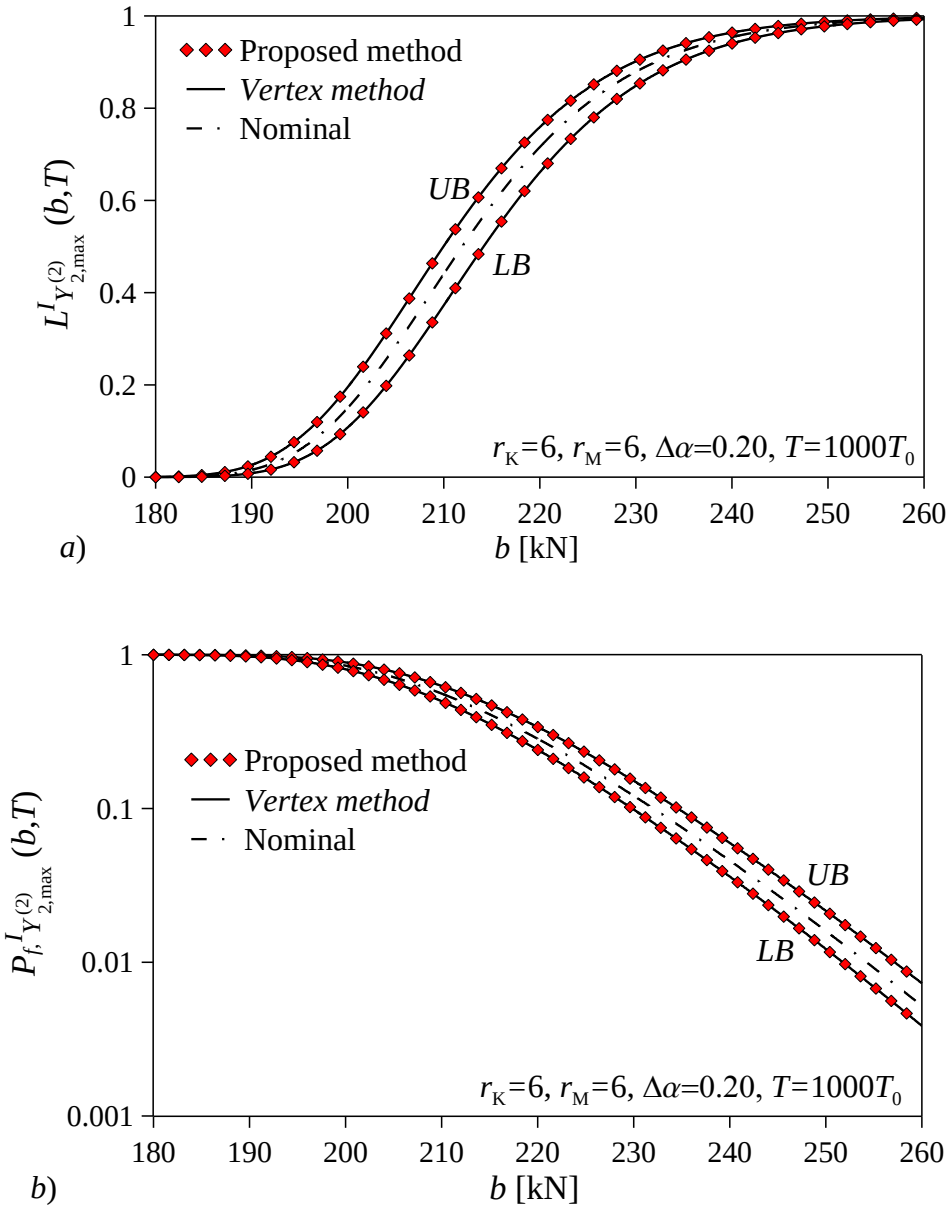


**Figure 15.** *UB* and *LB* of the a) *interval CDF* and b) *interval failure probability* of the *extreme value* shear stress process $Y^{(2)I}_{2,\max}(T)$ of the frame structure with uncertain Young's moduli $E^{(i)I} = E_0\left(1+\Delta\alpha\hat{e}^I_{(\mathrm{K})i}\right)$, $(i=1,2,3,4,5,10)$, and floor masses $m^{(i)I} = m_0\left(1+\Delta\alpha\hat{e}^I_{(\mathrm{M})i}\right)$, $(i=1,2,3,4,9,10)$: comparison between the proposed procedure, the *vertex method* $(\Delta\alpha=0.20)$ and the nominal solution.

**Figure 16**

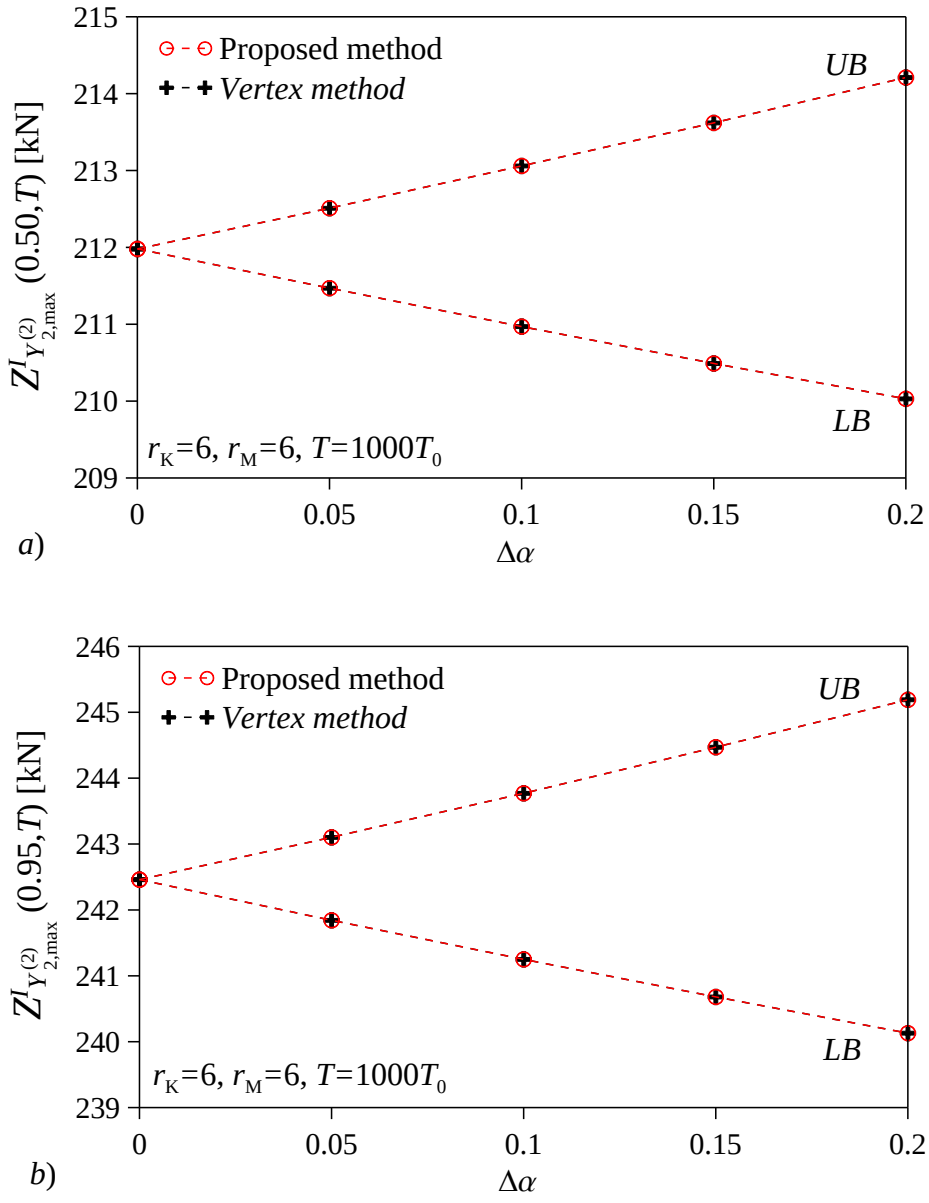


**Figure 16**. *UB* and *LB* of the *interval fractiles* of order $p=0.50$ a) and b) $p=0.95$ ($T=1000T_0$) of the *extreme value* shear stress process $Y^{(2)I}_{2,\max}(T)$ of the frame structure provided by the proposed procedure and the *vertex method* versus the deviation amplitude $\Delta\alpha$ of the interval Young's moduli $E^{(i)I}=E_0\left(1+\Delta\alpha\hat{e}^I_{(\mathrm{K})i}\right)$, $(i=1,2,3,4,5,10)$, and floor masses $m^{(i)I}=m_0\left(1+\Delta\alpha\hat{e}^I_{(\mathrm{M})i}\right)$, $(i=1,2,3,4,9,10)$.

**Figure 17**

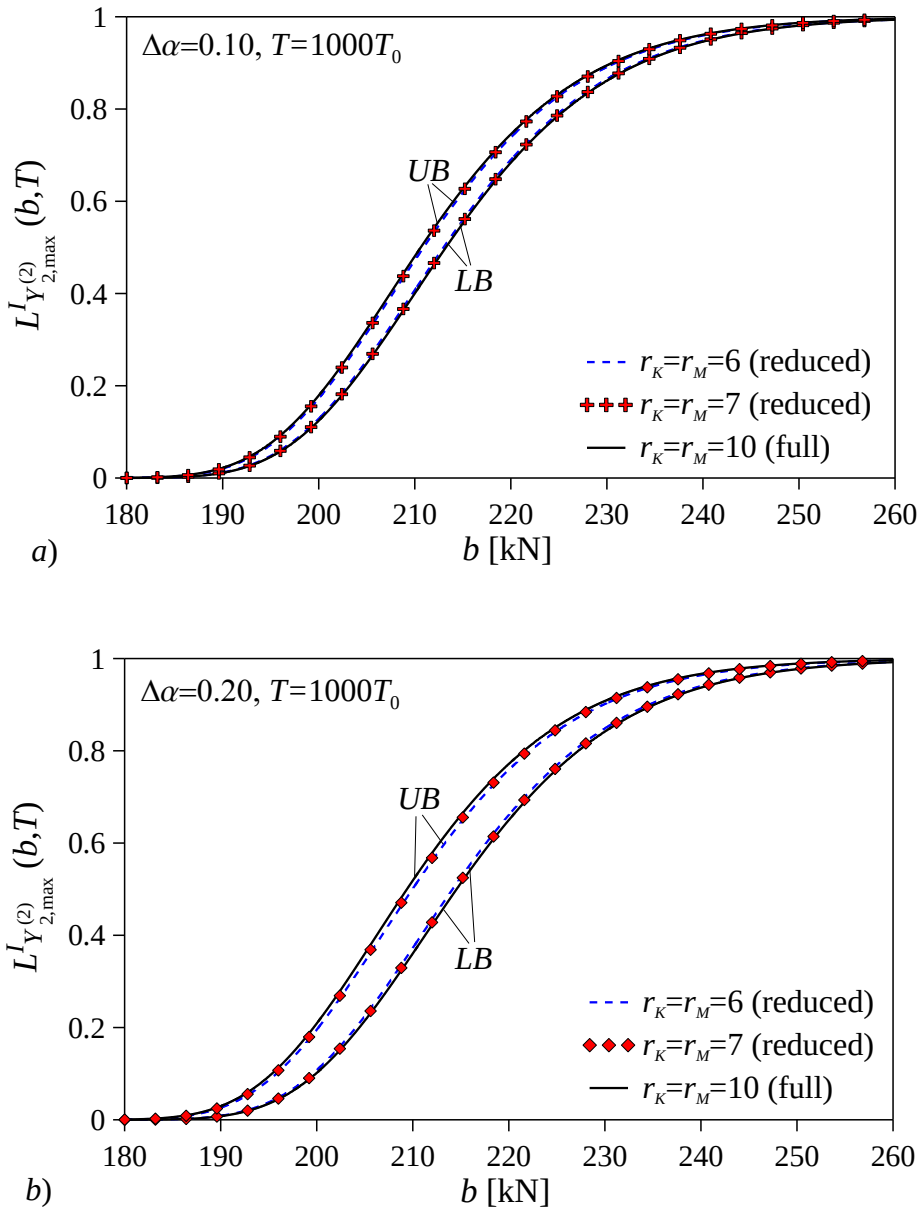


**Figure 17.** *UB* and *LB* of the *interval CDF* of the *extreme value* shear stress process $Y_{2,\max}^{(2)I}(T)$ of the frame structure provided by the proposed procedure considering all Young's moduli and floor masses as uncertain (full) and retaining only the first $r_{\mathrm{K}} = r_{\mathrm{M}} = 6$ and $r_{\mathrm{K}} = r_{\mathrm{M}} = 7$ most influential uncertain parameters (reduced): *a*) $\Delta\alpha = 0.10$ and *b*) $\Delta\alpha = 0.20$ ($T = 1000T_0$).